ORIGINAL PAPER

Data Mining and in Silico Analysis of Ethiopian Traditional Medicine: Unveiling the Therapeutic Potential of *Rumex abyssinicus* Jacq.

Lemessa Etana Bultum[1,2,3] · Gwangmin Kim[1,2] · Seon-Woo Lee[3] · Doheon Lee[1,2]

Abstract

Multicomponent traditional medicine prescriptions are widely used in Ethiopia for disease treatment. However, inconsistencies across practitioners, cultures, and locations have hindered the development of reliable therapeutic medicines. Systematic analysis of traditional medicine data is crucial for identifying consistent and reliable medicinal materials. In this study, we compiled and analyzed a dataset of 505 prescriptions, encompassing 567 medicinal materials used for treating 106 diseases. Using association rule mining, we identified significant associations between diseases and medicinal materials. Notably, wound healing—the most frequently treated condition—was strongly associated with *Rumex abyssinicus Jacq.*, showing a high support value. This association led to further in silico and network analysis of *R. abyssinicus* Jacq. compounds, revealing 756 therapeutic targets enriched in various KEGG pathways and biological processes. The Random-Walk with Restart (RWR) algorithm applied to the CODA PPI network identified these targets as linked to diseases such as cancer, inflammation, and metabolic, immune, respiratory, and neurological disorders. Many hub target genes from the PPI network were also directly associated with wound healing, supporting the traditional use of *R. abyssinicus* Jacq. for treating wounds. In conclusion, this study uncovers significant associations between diseases and medicinal materials in Ethiopian traditional medicine, emphasizing the therapeutic potential of *R. abyssinicus* Jacq. These findings provide a foundation for further research, including in vitro and in vivo studies, to explore and validate the efficacy of traditional and natural product-derived medicines.

Keywords Natural products · Drug discovery · Machine learning/Artificial intelligence · Molecular modeling

Introduction

Over time, numerous cultures worldwide have developed their own traditional healing systems. In recent years, there has been a significant increase in the popularity and acceptance of traditional, complementary, and alternative medicine (TCAM) in both developing and developed countries [1]. Traditional medicine (TM) is widely used and practiced in countries like China, Korea, India, and the African continent [2]. In China,

traditional herbal medicine accounts for 30–50% of the total medicinal consumption [3]. In African countries such as Ghana, Mali, Nigeria, and Zambia, herbal medicines are the primary treatment for ~60% of children with high fever caused by malaria [4]. This trend reflects the growing interest in natural product therapy and research on a global scale.

As a result of this increasing interest and utilization, there has been a corresponding rise in the availability of academic articles and electronic databases focusing on traditional medicines. An example of such a resource is the Compound Combination-Oriented Natural Product Database with Unified Terminology (COCONUT), which consolidates 21,456 oriental medicine prescriptions from Korean, Chinese, and Japanese herbal medicine sources [5]. Additionally, the integrated Ethiopian traditional herbal medicine and phytochemicals database (ETM-DB) encompasses details on 573 multi-component prescriptions derived from combinations of 265 medicinal materials found in Ethiopia [6]. The ETM-DB serves as a valuable resource to augment the knowledge and utilization of traditional medicines in Ethiopia, primarily focusing on their application in natural product-based drug

✉ Lemessa Etana Bultum
  leme3388@gmail.com

✉ Doheon Lee
  dhlee@kaist.ac.kr

[1] Department of Bio and Brain Engineering, Korea Advanced Institute of Science and Technology (KAIST), Daejeon, South Korea

[2] Bio-Synergy Research Center, Daejeon, South Korea

[3] Institute of Agricultural Life Sciences, Dong-A University, Busan, South Korea

discovery. These databases serve to consolidate and disseminate knowledge, supporting research in natural product-based therapies globally.

To harness the power of the vast and diverse data, several key computational techniques have emerged. Coupled with massive computing resources and extensive virtual libraries of drug-like molecules, these developments are reshaping how we approach drug discovery [7]. Computational drug discovery, also known as in silico drug discovery, employs two primary methodologies: Virtual Screening (VS) and Ligand-Based Drug Design (LBDD), each leveraging computational techniques to accelerate the identification and design of therapeutic compounds [8–10]. VS utilizes computational models to analyze extensive compound libraries and predict their ability to bind with target biomolecules associated with diseases. This method helps prioritize compounds based on their predicted binding affinities, guiding further experimental validation [11]. Conversely, LBDD relies on computational models built upon known ligands to design new compounds that mimic their structures or properties, aiming to interact effectively with the target [9]. Both methodologies incorporate techniques such as Quantitative Structure-Activity Relationship (QSAR) modeling to predict biological activities and optimize compounds for efficacy and safety profiles [12]. Additionally, Machine Learning/Artificial Intelligence (ML/AI) methods form another category within computational drug discovery [13, 14]. These methods employ predictive modeling to forecast biological activities or adverse effects of compounds, uncovering patterns and correlations crucial for drug discovery. Data mining is one of the ML methods that could be utilized to effectively handle and analyze large datasets and convert into useful knowledge for various decision making. Data mining is the process of extracting implicit, previously unknown, and potentially useful information from data ([15, 16, 17]).

Association rule mining is a fundamental data mining concept extensively investigated to identify associations between itemsets in vast databases. Its objective is to identify sets of items that frequently occur together in transactional databases. The association rule mining algorithm was first introduced by Agrawal et al., [18], primarily applied to analyze basket data models, where each basket represents a transaction, and the items purchased within the basket are termed as itemsets. Network analysis is another crucial approach that leverages computational technologies to support drug discovery efforts. Biological networks, which represent complex systems of interacting entities, can be categorized into several types, including Protein-Protein Interaction (PPI) networks, signal transduction networks, and gene regulatory networks. To analyze these networks, various methods and algorithms are employed, including centrality measures, community detection, and pathway analysis. The Random - Walk with Restart (RWR) algorithm is particularly valuable for identifying key nodes and functional modules within networks and is often applied to centrality measures and community detection. RWR simulates a stochastic process where a "walker" traverses the nodes of a graph, occasionally returning to the starting point, which aids in exploring the network's structure and revealing important relationships and functions [19].

Ethiopia is rich in cultural diversity, encompassing over 80 ethnic groups, each with unique traditions and knowledge in traditional healthcare. The country's history is deeply intertwined with the use of traditional medicine, which encompasses a wide range of practices, including preventive, curative, and even surgical methods, showcasing the diverse and vibrant Ethiopian cultures [20]. According to the New Partnership for Africa's Development, a significant portion of the Ethiopian population, estimated between 60 and 79%, still relies on indigenous traditional medicine for their healthcare needs [21]. This continuing reliance on traditional medicine can be attributed to various factors. As a developing nation, access to modern healthcare remains limited in many parts of the country. Moreover, the expenses associated with modern medical services make them unaffordable for many people. In contrast, traditional practices are more familiar and culturally accepted, leading to their continued usage. Beyond the cultural significance, Ethiopia's natural resource abundance contributes to the popularity of traditional medicine practices. The country is blessed with a remarkable diversity of flora, including 6500–7000 floral species, of which 10–12% are exclusive to Ethiopia. Remarkably, more than 1000 plant species, accounting for 15% of the total flora, are utilized for medicinal purposes [22–24]. In this way, Ethiopia's heritage, cultural acceptance, and abundant natural resources all converge to sustain the utilization of traditional medicine, bridging the gap in healthcare access and meeting the needs of its people.

Traditional medicine in Ethiopia holds significant cultural and health importance, drawing knowledge from diverse sources including ancient records and oral traditions [24]. Indigenous practitioners pass down this wisdom, forming the foundation of Ethiopian traditional literature. Academic research complements this by exploring ethnobotany, ethnomedicine, phytochemistry, and the biological properties of medicinal plants [6, 25]. This heritage plays a pivotal role in Ethiopian society, deeply embedded in its cultural, social, and economic fabric over centuries. Particularly in rural and remote areas with limited access to modern healthcare, traditional medicine serves as a readily accessible and affordable alternative. Its holistic approach, addressing physical, spiritual, and emotional well-being, resonates with local beliefs in comprehensive healthcare. Increasingly recognized for its role alongside modern

healthcare, traditional medicine supports chronic disease management and palliative care. Ethiopia's rich biodiversity provides an abundant source of medicinal plants crucial for traditional remedies, preserving both natural resources and local livelihoods through sustainable practices. Beyond national borders, Ethiopian traditional medicine attracts global interest for its potential contributions to global health solutions. In summary, Ethiopian traditional medicine embodies cultural preservation, community health, and sustainable practices, offering insights and solutions that resonate locally and internationally [26, 27].

Ethiopian traditional medicine, like other traditional systems such as oriental medicine, predominantly involves the use of multicomponent prescriptions. These practices recognize the synergistic interactions and potentiating effects among the various medicinal materials used in prescriptions [28]. However, the available information on the therapeutic use of multicomponent prescriptions remains limited, despite the relatively abundant modern literature on the therapeutic use of individual medicinal materials. It is evident in Ethiopia, as well as in other countries and regions of the world, including India [29], that the presence of diverse cultures and ethnic groups with their own traditional medicine practices leads to variations in prescriptions and constituent medicinal materials for similar symptoms. These prescriptions vary among different traditional medicine practitioners, influenced by cultural practices and geographical locations. Additionally, the availability of specific medicinal materials for prescriptions is influenced by the geo-climatic conditions of a given area, further contributing to these variations.

These variations in traditional medicine practices lead to challenges in establishing a consistent and reliable selection of therapeutic medicinal materials and developing effective prescriptions for treating prevalent diseases. The lack of standardization not only complicates scientific validation but also poses challenges in ensuring the safety and efficacy of treatments, potentially leading to unpredictable outcomes [30, 31]. These challenges have significantly hindered the development of reliable therapeutic medicines, creating barriers to the systematic study and clinical testing needed for modern drug development. To address these issues and promote harmonized practices, standardizing traditional medicine practices through systematic analysis and harmonization is crucial. Our approach in this study aims to identify consistent and reliable medicinal materials, which can then be developed into standardized therapeutic agents. Such an approach not only acknowledges the cultural significance of traditional medicine but also enhances its credibility and applicability in contemporary medical practice.

In this study, we employed data mining and network analysis techniques to analyze prescription data, aiming to establish a reliable collection of medicinal materials for practitioners by identifying associations between common diseases and these medicinal materials. Furthermore, we conducted in silico and network analysis to support these associations and affirm the traditional therapeutic uses of medicinal materials. This included molecular-level investigations to uncover therapeutic targets, pathways, biological processes, and disease associations, exemplified by our analysis of *Rumex abyssinicus* Jacq. (Polygonaceae) and its application in wound healing. By compiling and analyzing traditional medicine data in this manner, our study fills a gap in research by providing comprehensive insights into Ethiopian traditional medicine prescription and supports the development of harmonized and effective natural product-derived medicines.

Material and Methods

Compilation and Pre-Processing of Traditional Medicine Prescriptions

Multicomponent traditional medicine prescriptions, derived from natural products, are widely practiced in Ethiopia. Despite substantial literature existing on the therapeutic use of individual medicinal materials, information about the uses of multicomponent prescriptions is limited. For this study, prescription data were manually curated from various sources including research articles, books, and natural product databases. The majority of the prescription data was compiled from the book "Medicinal Plants and Enigmatic Health Practices of Northern Ethiopia" [32], which is the most comprehensive source containing extensive records of traditional multicomponent medicine prescriptions from northern Ethiopia. Authored by expert traditional medicine practitioners, the book draws from comprehensive sources including ancient manuscripts and microfilms from the British Library, which were taken from Ethiopia long ago. Additional prescription information was sourced from research articles focusing on detailed prescriptions from diverse regions of Ethiopia [33–35] and the natural product database, ETM-DB [6].

Despite the scarcity of information on the therapeutic uses of multicomponent prescriptions, the dataset we compiled is sufficient to draw conclusions regarding patterns in medicinal material usage within traditional medicine prescriptions. In this study, prescriptions were selected if they included the use of multicomponent medicinal materials for treating human diseases. To ensure data relevance and specificity, prescriptions for non-illness practices (e.g., remedies for the evil eye, attack deterrents, love potions, and intelligence boosters) were excluded from the dataset. Furthermore, diseases with a limited number of prescriptions and associated medicinal materials were excluded to

Fig. 1 Overview of the process to identify associations between medicinal materials and human diseases from prescription data. Multicomponent prescriptions, constituent medicinal materials, and related diseases were organized in a transaction database. Association rule mining was then employed to extract significant associations between medicinal materials and diseases from the multicomponent prescriptions
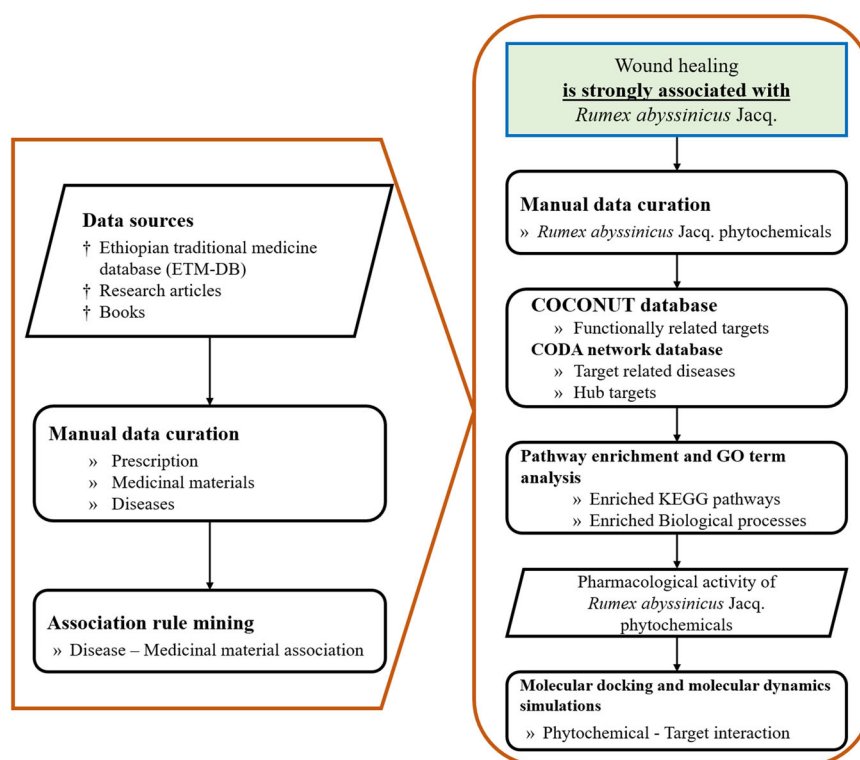
facilitate effective association rule analysis. The study focused on diseases with a substantial number of prescriptions and diverse types of medicinal materials across prescriptions to identify and analyze consistent medicinal materials for each disease. As a result, the dataset used in this study comprised 505 prescriptions involving combinations of 567 medicinal materials used to treat 106 distinct human diseases.

To conduct association rule mining and identify significant associations between medicinal materials and diseases, we constructed a binary matrix. Each prescription was represented as a row in the matrix, with columns corresponding to human diseases and medicinal materials. The presence of a medicinal material in a prescription was denoted by "1", while its absence was denoted by "0".

After identifying significant associations between diseases and medicinal materials, we conducted an in silico analysis, focusing on *R. abyssinicus* Jacq. This analysis involved integrating data on the phytochemical constituents of *R. abyssinicus* Jacq. and therapeutic targets from databases such as the Integrated Ethiopian Traditional Herbal Medicine and Phytochemicals Database (ETM-DB) [6] and the Compound Combination-Oriented Natural Product Database with Unified Terminology (COCONUT) [5]. We explored pathways and biological processes using Kyoto Encyclopedia of Genes and Genomes (KEGG) pathways [36] and The Gene Ontology (GO) database and informatics resource [37].

Additionally, we conducted network analysis by applying the Random- Walk with Restart (RWR) algorithm within the CODA network to identify diseases associated with these targets. Furthermore, we constructed a Protein-Protein Interaction (PPI) network using the CODA network to identify hub targets linked to the phytochemicals. Subsequently, molecular docking and molecular dynamics simulations were carried out to investigate the interactions between the phytochemicals and the identified hub targets, providing deeper insights into their potential therapeutic effects.

Figure 1 outlines the research process from data collection and association rule mining to identify relationships between diseases and medicinal materials. It also depicts the subsequent in silico and network analysis used to explore the therapeutic effects of *R. abyssinicus* Jacq. phytochemicals.

Association Rule Mining

Association Rule Mining is a key data mining technique used to identify frequent itemsets and their associations in large databases. Originally introduced by Agrawal et al. [18] for analyzing basket data models, it identifies sets of items that frequently occur together in transactions. In this study, we adopted the association rule mining algorithm from Agrawal et al., using user-defined minimum support and confidence thresholds to generate relevant association rules.

For an association rule X (antecedent) $\Rightarrow$ Y (consequent), the support of the rule is calculated as the proportion of transactions in the data that contain both antecedent and

consequent, representing the frequency of occurrence of the rule.

$$\text{Support}(X \Rightarrow Y) = \frac{\text{Number of transactions containing both } X \wedge Y}{\text{Total number of transactions}}$$

Confidence is a measure of how often a rule is true in the data. It is the ratio of the number of transactions that contain both the antecedent and the consequent of the rule, to the number of transactions that contain only the antecedent [38]. A high confidence means that the rule is reliable and consistent. A confidence value of 0 indicates that none of the transactions with the antecedent itemset have the consequent itemset, while a confidence value of 1 signifies that all transactions with the antecedent itemset include the consequent itemset.

$$\text{Confidence}(X \Rightarrow Y) = \frac{\text{Number of transactions containing both } X \wedge Y}{\text{Number of transactions containing } X}$$

Lift is a measure of how much more likely the consequent of a rule is to occur when the antecedent is present, compared to when it is absent. It is the ratio of the confidence of the rule, to the frequency of the consequent in the whole dataset [39]. For example, for the association rule X (antecedent) $\Rightarrow$ Y (consequent), the lift is the confidence of the rule, divided by the proportion of transactions that have Y. A high lift value indicates a significant and interesting rule, highlighting a strong association between the antecedent and the consequent. The lift value of 1 means that antecedent and consequent itemsets are completely independent, which can be achieved by the pure random rules, and the lift value of 2 means that antecedent and consequent itemsets are two times more dependent than the pure random rules [39].

When configuring the association rule parameters for this specific analysis, the support of an item (either disease or medicinal material) is determined by the fraction of transactions (in this context, prescriptions) in which the item is present. The support value of an association rule is calculated as the ratio of the number of prescriptions containing both the disease and medicinal materials to the total number of prescriptions. The confidence value of an association rule is calculated as the ratio of prescriptions that include both the disease and the medicinal material to the prescriptions that include the disease alone. This value provides an indication of how often the rule has been observed to be true. The lift is a measure of how much more likely the medicinal material occurs when the related disease is present, compared to when the disease is absent [41]. It indicates the dependence between the disease and medicinal material. In this analysis, a high lift value and lower confidence suggest that the medicinal material is specifically used for treating that particular disease. On the other hand, a high confidence value and relatively low lift value indicate that the medicinal material is not specific to the disease, and it is utilized to treat various diseases in addition to the associated disease.
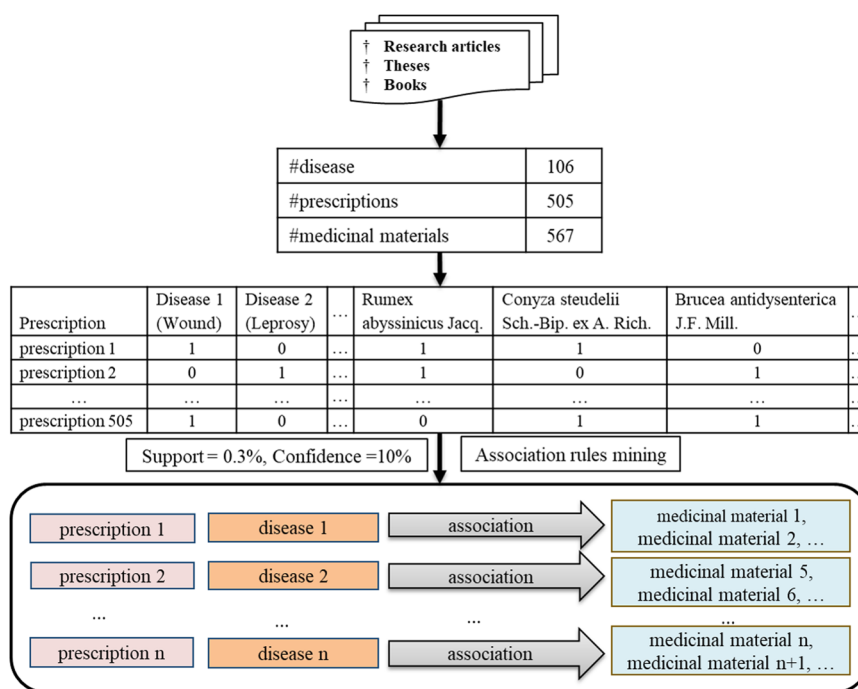
Figure 2 provides an overview of the process used to identify associations between medicinal materials and human diseases from prescription data. It shows how multicomponent prescriptions, constituent medicinal materials, and related diseases were organized in a transaction database. Association rule mining was then applied to extract significant associations between medicinal materials and diseases from these multicomponent prescriptions.

$$\text{lift}(X \Rightarrow Y) = \frac{(\text{Number of transactions containing both } X \wedge Y)/(\text{Number of transactions containing } Y)}{\text{Fraction of transactions containing } Y}$$

In this study, association rule mining was employed to identify the associations between diseases and therapeutic medicinal materials using the *arules* package with the *apriori* algorithm in R [40]. The association rules took the form of "antecedent $\Rightarrow$ consequent", where the antecedent represented the disease and the consequent represented the medicinal material. Statistical parameters, including support, confidence, and lift, were used to assess the significance of the associations. In this analysis, we set minimum support and confidence thresholds of 0.3 and 10%, respectively. Any generated rule that met or exceeded these thresholds for both support and confidence was deemed statistically significant.

Network Visualization of Associations between Traditional Medicine and Diseases

In our analysis, we represented disease and medicinal materials as nodes in a bipartite network, where edges indicate that the medicinal material is part of the prescription used to treat the disease. By employing the Python NetworkX library version 2.5, we constructed, analyzed, and visualized the networks, allowing for a better understanding and visualization of the associations between the interacting items.

To further elucidate these associations, radar charts were employed to visually interpret the association rules between

Fig. 2 Process for identifying associations between medicinal materials and diseases. It shows the organization of prescription data in a transaction database and the application of association rule mining to reveal significant associations

	Research articles
†	Research articles
†	Theses
†	Books

#disease	106
#prescriptions	505
#medicinal materials	567

Prescription	Disease 1 (Wound)	Disease 2 (Leprosy)	...	Rumex abyssinicus Jacq.	Conyza steudelii Sch.-Bip. ex A. Rich.	Brucea antidysenterica J.F. Mill.	...
prescription 1	1	0	...	1	1	0	...
prescription 2	0	1	...	1	0	1	...
...	...	...	...	...	...	...	...
prescription 505	1	0	...	0	1	1	...

Support = 0.3%, Confidence =10% | Association rules mining

prescription 1	disease 1	association	medicinal material 1, medicinal material 2, ...
prescription 2	disease 2	association	medicinal material 5, medicinal material 6, ...
...	...	...	...
prescription n	disease n	association	medicinal material n, medicinal material n+1, ...

diseases and medicinal materials. These charts effectively present multidimensional data, allowing for a comparison of statistical measures such as confidence and lift across various disease-medicinal material pairs [42]. Radar charts illustrated confidence values for different medicinal materials for selected diseases, depicted lift values indicating the specificity of associations, and presented standardized values for comparative analysis. This visual representation complemented the quantitative analysis by providing insights into the relative significance of medicinal materials in treating specific diseases.

Exploring *R. abyssinicus* Jacq. Phytochemicals' Pharmacological Activity Through Target Identification, Network Analysis, KEGG Pathways, and GO Terms

In our study, we explored the pharmacological potential of phytochemicals from *R. abyssinicus* Jacq., with a focus on their therapeutic targets and related pathways [43]. Mukherjee et al., [43]. We specifically targeted *R. abyssinicus* Jacq. because of its notable association with wound healing, as detailed in Table 1.

The process outlined in Fig. 3 involved several key steps. First, we compiled phytochemical constituents from sources such as the ETM-DB [6] and relevant literature. Next, we identified functionally related therapeutic targets using the COCONUT database [5], which includes information on traditional herbal medicines, combination drugs, functional foods, and molecular drug/target interactions.

We then constructed a heterogeneous network using the CODA network [44]. Using the RWR algorithm [19], we traced the information flow from therapeutic targets to disease nodes. The RWR algorithm helped us prioritize disease nodes based on their connectivity to the therapeutic targets. Finally, the disease nodes were ranked according to their RWR scores, providing insights into which diseases are most closely associated with the identified targets.

To further understand the interactions of *R. abyssinicus* Jacq. phytochemicals with biological systems, we analyzed the Kyoto Encyclopedia of Genes and Genomes (KEGG) pathway enrichment [36] and Gene Ontology (GO) terms [37] associated with the identified targets. We conducted Gene Set Enrichment Analysis (GSEA) [45] using the enrichr function in the Gseapy Python library (https://www.gsea-msigdb.org/gsea/index.jsp), with gene sets "KEGG_2021_Human", and "GO_Biological_Process_2021" applying a cut-off of 0.5. This analysis assessed the association of phytochemicals with predefined biological pathways, providing valuable insights into their potential pharmacological effects.

Integration of PPI Network Analysis, Protein-Ligand Interactions, and MD Simulation in Investigating *R. abyssinicus* Jacq. Phytochemicals

We constructed a Protein-Protein Interaction (PPI) network using the Context-Oriented Directed Associations (CODA) network, which integrates data from multiple sources including BioGRID, KEGG, and EndoNet. The BioGRID data (release 4.4.198) was obtained from https://downloads.

Table 1 Associations between diseases and medicinal materials, including support, confidence, and lift values

Disease	Medicinal Material	Support (%)	Confidence (%)	Lift
Wound	*Rumex abyssinicus* Jacq.	1.39	17.95	5.33
	Conyza steudelii Sch.-Bip. ex A. Rich.	1.19	15.38	5.55
	Plumbago zeylanica L.	0.99	12.82	2.02
	Calpurnia aurea (Ait.) Benth.	0.79	10.26	2.35
Mental illness	*Clerodendrum myricoides* (Hochst.) R. Br. ex Vatke	1.58	29.63	3.48
	Ruta chalepensis L.	1.19	22.22	3.87
	Clausena anisata (Willd.) Benth.	0.79	14.81	4.68
	Trigonella foenum-graecum L.	0.59	11.11	7.01
	Cannabis sativa L.	0.59	11.11	5.10
	Withania somnifera (L.) Dunal	0.59	11.11	2.81
	Gladiolus psittacinus Hook.	0.59	11.11	3.74
	Verbena officinalis L.	0.59	11.11	2.95
	Lepidium sativum L.	0.59	11.11	2.95
	Asparagus africanus Lam.	0.59	11.11	2.44
	Securidaca longepedunculata Fresen.	0.59	11.11	2.44
	Capparis tomentosa Lam.	0.59	11.11	2.67
	Adhatoda schimperiana (Hochst) Nees.	0.59	11.11	2.34
	Myrrh (*Commiphora cf. crenulata* or other *C. spp.*)	0.59	11.11	2.08
	Cucumis ficifolius A. Rich.	0.59	11.11	1.22
Sexual stimulation (aphrodisiacs)	*Tragia pungens* (Forssk.) Muell. Arg.	1.19	33.33	28.06
	Asparagus africanus Lam.	0.99	27.78	23.38
	Ferula communis L.	0.99	27.78	9.35
	Thalictrum rhynchocarpum Dill. & A. Rich.	0.79	22.22	4.32
	Phoenix reclinata Jacq.	0.59	16.67	7.65
	Sida cuneifolia Roxb.	0.59	16.67	7.01
	Olea europaea L. subsp. *africana* (Mill.) P.S. Green	0.59	16.67	6.47
	Gladiolus psittacinus Hook.	0.59	16.67	5.61
	Cucumis ficifolius A. Rich.	0.59	16.67	1.83
	Habenaria sp.	0.40	11.11	28.06
	Sida cuneifolia Roxb. or *S. ovata* Forssk.	0.40	11.11	9.35
	Tragia pungens (Forssk) Muell. Arg.	0.40	11.11	8.02
	Catha edulis (Vahl) Forssk. ex Endl.	0.40	11.11	9.35
	Stylochiton kerensis N.E. Brown	0.40	11.11	6.23
	Cannabis sativa L.	0.40	11.11	5.10
	Zehneria scabra (L.f.) Sonder	0.40	11.11	2.67
	Clerodendrum myricoides (Hochst.) R. Br. ex Vatke	0.40	11.11	1.30
Eye disease	*Hagenia abyssinica* (Bruce) J.F. Gmel.	0.59	18.75	7.28
	Premna schimperi Engl.	0.40	12.50	9.02
	Artemisia afra Jacq. ex Willd.	0.40	12.50	7.89
	Vitis vinifera L.	0.40	12.50	5.74
	Solanum marginatum L.f.	0.40	12.50	5.26
Rabies	*Cucumis ficifolius* A. Rich.	1.39	43.75	4.80
	Phytolacca dodecandra L'Herit.	0.99	31.25	10.52

Table 1 (continued)

Disease	Medicinal Material	Support (%)	Confidence (%)	Lift
	Cyphostemma junceum (Webb) Descoings ex Wild & Drummond	0.79	25.00	10.52
	Solanum cf. adoense Hochst.	0.79	25.00	4.86
	Adhatoda schimperiana (Hochst) Nees.	0.59	18.75	3.95
	Sida cuneifolia Roxb. or *S. ovata* Forssk.	0.40	12.50	10.52
	Senecio myriocephalus Sch. Bip. ex A.Rich.	0.40	12.50	7.01
	Vitis vinifera L.	0.40	12.50	5.74
	Kalanchoe petitiana A. Rich.	0.40	12.50	5.74
	Mandragora officinarum/Luffa aegyptica	0.40	12.50	4.86
Frequent miscarriage	*Osyris quadripartita* Decne.	0.59	18.75	5.57
	Clutia abyssinica Jaub. & Spach.	0.59	18.75	6.31
	Solanum cf. adoense Hochst.	0.59	18.75	3.64
	Cucumis ficifolius A. Rich.	0.59	18.75	2.06
	Periploca linearifolia A. Rich. & Quart.-Dill.	0.40	12.50	10.52
	Aloe sp.	0.40	12.50	6.31
	Rumex nervosus Vahl	0.40	12.50	4.86
Leprosy	*Plumbago zeylanica* L.	0.99	33.33	5.26
	Withania somnifera (L.) Dunal	0.59	20.00	5.05
	Euclea schimperi (DC.) Dandy	0.59	20.00	5.61
	Capparis tomentosa Lam.	0.59	20.00	4.81
	Sylvicapra grimmia	0.40	13.33	16.83
	Maesa lanceolata Forssk.	0.40	13.33	22.44
	Ranunculus multifidus Forssk.	0.40	13.33	22.44
	Olea europaea L. subsp. *africana* (Mill.) P.S. Green	0.40	13.33	5.18
	Osyris quadripartita Decne.	0.40	13.33	3.96
	Clematis simensis Fresen.	0.40	13.33	5.18
	Brucea antidysenterica J.F. Mill.	0.40	13.33	3.96
	Rumex abyssinicus (Jacq.).	0.40	13.33	3.54
	Jasminum floribundum R. Br. ex Fresen.	0.40	13.33	3.06
	Acokanthera schimperi (DC.) Oliv.	0.40	13.33	3.21
	Cucumis ficifolius A. Rich.	0.40	13.33	1.46
Eczema	*Hagenia abyssinica* (Bruce) J.F. Gmel.	0.59	21.43	8.32
	Cucumis ficifolius A. Rich.	0.59	21.43	2.35
	Lichen	0.40	14.29	14.43
	Gossypium barbadense L.	0.40	14.29	12.02
	Mandragora officinarum/Luffa aegyptica	0.40	14.29	5.55
	Zehneria scabra (L.f.) Sonder	0.40	14.29	3.44
Menorrhagia	*Brassica nigra* L.	0.59	21.43	12.02
	Protea gaguedi Gmel.	0.40	14.29	36.07
	Cordia africana Lam.	0.40	14.29	10.31
	Nigella sativa L.	0.40	14.29	6.56
	Achyranthes aspera L.	0.40	14.29	3.61
	Asparagus africanus Lam.	0.40	14.29	3.14
Malaria	*Dodonaea viscosa* (L.) Jack.	0.59	25	15.78
	Ekebergia capensis Sparm.	0.4	16.67	12.02

Table 1 (continued)

Disease	Medicinal Material	Support (%)	Confidence (%)	Lift
	Kanahia laniflora (Forssk.) R. Br.	0.4	16.67	7.65
	Jasminum floribundum R. Br. ex Fresen.	0.4	16.67	3.83
	Solanum cf. adoens Hochst.	0.4	16.67	3.24
	Clerodendrum myricoides (Hochst.) R. Br. ex Vatke	0.4	16.67	1.96

Fig. 3 Schematic overview of the methods for identifying potential therapeutic activities of *R. abyssinicus* Jacq. phytochemicals. This process involves compiling phytochemical data from various sources, identifying therapeutic targets using the COCONUT database, constructing a heterogeneous network, and identifying related diseases and hub targets with the CODA network. Pathway enrichment analysis was performed using KEGG and GO terms, followed by molecular docking and molecular dynamics simulations to characterize phytochemical-target interactions
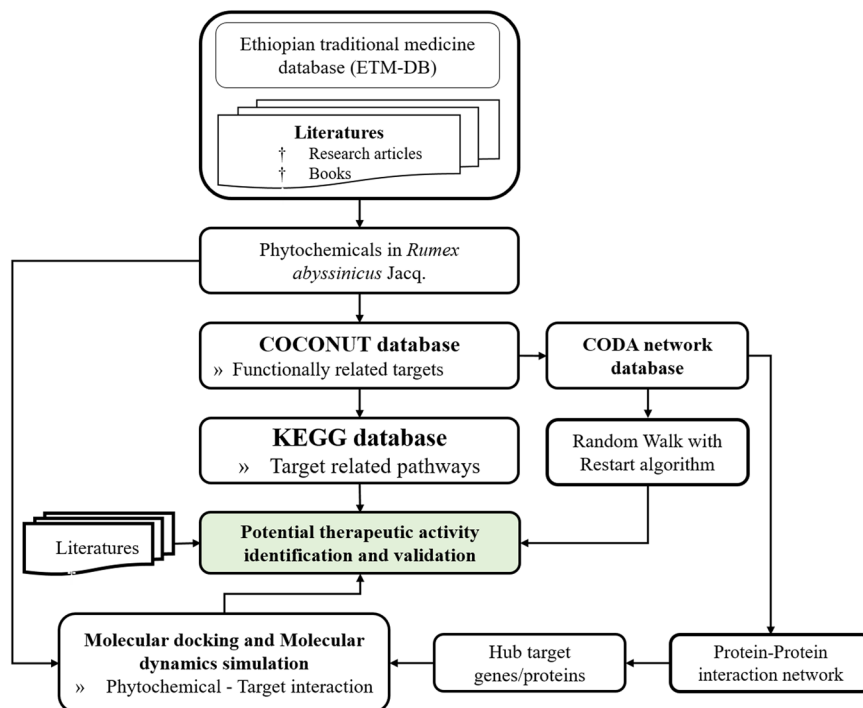
thebiogrid.org/BioGRID. For KEGG, we used the REST API available at http://rest.kegg.jp/ to retrieve XML format text files, which we processed to filter protein-protein interactions and convert them into Entrez IDs. Additionally, we accessed data from EndoNet at http://endonet.bioinf.med.uni-goettingen.de in XML format. These data sources were combined, and overlapping interactions were removed. The cleaned data was then used to construct the PPI network with the Python library NetworkX 2.5. The final PPI network comprises 17,358 protein nodes and 261,334 edges.

To focus on therapeutic targets related to *R. abyssinicus* Jacq. phytochemicals, we selected proteins with gene product relationships from this PPI network. We converted the nodes into gene symbols for clarity. From this network, we extracted a hub network highlighting therapeutic targets associated with *R. abyssinicus* Jacq. phytochemicals. Hub targets were identified using two network measures: degree centrality and eigenvector centrality, with hub targets defined as nodes within the top 1% for both measures.

We then performed structure-based molecular docking to evaluate the binding interactions between the phytochemicals and their associated hub targets. For this analysis, we retrieved PDB files for five selected hub proteins from the RCSB Protein Data Bank (https://www.rcsb.org/) and obtained the 3D SDF files of the ligands from the PubChem database [46]. Protein-ligand docking was conducted using the CB-Dock web server (https://cadd.labshare.cn/cb-dock2/index.php), which integrates cavity detection, docking, and homologous template matching. CB-Dock utilizes AutoDock Vina [47]. Finally, we visualized the 3D protein-ligand complexes using CB-Dock, which provides interactive 3D visualizations of the binding modes. We also exported images of these complexes directly from the CB-Dock web server.

Following the molecular docking studies, we conducted Molecular Dynamics (MD) simulations to assess the stability of the binding interactions between the phytochemicals and their target proteins. Emodin, which exhibited a relatively low binding energy score of -8.9 kcal/mol with the

target protein ESR1 in docking studies, was selected for the MD simulation. We performed a 100 nanosecond (ns) simulation using the GROningen MAchine for Chemical Simulations (GROMACS) 2021.4 software package [48]. For protein topology preparation, we used SwissParam (https://www.swissparam.ch/) [49], and for ligand topology preparation, we employed the CHARMM27 all-atom force field [50]. The simulation utilized a triclinic box with the Simple Point Charge (SPC) water model and explicit solvent periodic boundary conditions. Charge neutralization of the solvated complexes was achieved with sodium and chloride ions. Energy minimization was performed using the steepest descent method over 5000 steps to eliminate any steric clashes and bad contacts.

A series of equilibration steps followed to relax the system and bring it to an appropriate starting state. This included using a Berendsen thermostat for equilibration under constant Number of particles, Volume, and Temperature (NVT) for 100 picoseconds (ps) [51]. Re-equilibration was carried out with a Parrinello-Rahman barostat, applying a time step of 2 femtoseconds (fs) for each equilibration round over a further 100 ps at constant Number of particles, Pressure, and Temperature (NPT) [52]. The MD production phase was conducted for 100 ns with a time step of 2 fs, maintaining a constant temperature of 300 K and pressure of 1 atm. Using GROMACS' "trjconv" function, the complex was re-centered and re-wrapped into the unit cells for trajectory analysis. The Root Mean Square Deviation (RMSD) of the protein, ligand, and protein-ligand complex relative to their initial positions, as well as the Radius of gyration (Rg), were used to analyze the trajectories. Data visualization and charting was done using the Grace: GRaphing, Advanced Computation and Exploration of data [53], available at https://plasma-gate.weizmann.ac.il/Grace/.

Results and Discussion

Associations between Disease and Medicinal Materials

In this study, we used the a priori algorithm of association rule mining to identify significant associations between diseases and medicinal materials in Ethiopian traditional medicine prescriptions. We assessed these associations using statistical metrics such as support, confidence, and lift. Table 1 presents the support, confidence, and lift values for the association rules between the top ten most frequently treated diseases and their associated medicinal materials, with a focus on rules with a confidence value of at least 10%. For a more comprehensive overview, Supplementary Table S1 online includes all identified associations between

diseases and medicinal materials, along with their support, confidence, and lift values.

To illustrate our findings, we selected particular diseases and their associated medicinal materials based on the frequency of prescriptions. Figure 4 presents a bar chart depicting the frequency of the most commonly treated diseases in our dataset. This chart highlights wound healing as the most prevalent health concern addressed by traditional medicine practitioners. Each bar in the chart represents a specific disease, with its height indicating the number of prescriptions for that disease. Following wound healing, other common conditions include mental illness, sexual stimulation (aphrodisiacs), eye disease, rabies, frequent miscarriage, leprosy, eczema, menorrhagia, malaria, epidemic, rectal prolapse, syphilis, rheumatic pain, sorcery poisoning (stomach infection), migraine, epilepsy, hemorrhoids, oxytocics, cough, infertility, deafness, Ascaris, vitiligo, headache, relapsing fever, snake bite, scabies, measles, and haematuria.

The use of the a priori algorithm allowed us to systematically identify these significant associations, and Table 1 provides a detailed overview of the association rules derived from our analysis.

The significance of the association rules in this study is evaluated using lift and confidence values. Significant associations are indicated by high values of confidence and lift. For instance, the rule wound ⇒ *Rumex abyssinicus* Jacq. shows a high confidence value of 17.95 and a lift value of 5.33. This suggests that *R. abyssinicus* Jacq. is frequently used for treating wounds in traditional medicine. Supporting this, Mulisa et al. [54] demonstrated the wound healing and anti-inflammatory properties of *R. abyssinicus* Jacq. This finding underscores how association rules can
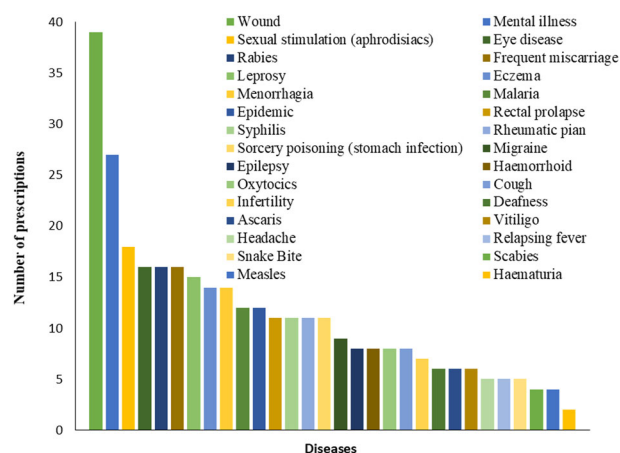

Fig. 4 Frequency of various conditions treated with traditional medicine. This bar chart illustrates the prevalence of different conditions addressed by traditional medicine practitioners in the dataset used in this study

identify key medicinal materials, while additional experimental research can validate their traditional uses.

In contrast, the rules Mental illness ⇒ *Clerodendrum myricoides* (Hochst.) R. Br. ex Vatke. and Mental illness ⇒ *Ruta chalepensis* L. exhibit high confidence but relatively low lift values. This indicates that these medicinal materials are frequently used to treat mental illness, but they are also commonly applied to other health conditions. On the other hand, the rule Mental illness ⇒ *Trigonella foenum-graecum* L. has relatively higher lift value of 7.01 and a lower confidence value of 11.11, suggesting that *T. foenum-graecum* L. is more specifically associated with treating mental illness.

For the category of sexual stimulation (aphrodisiacs), the rules Sexual stimulation (aphrodisiacs) ⇒ *Tragia pungens* (Forssk.) Muell. Arg., Sexual stimulation (aphrodisiacs) ⇒ *Asparagus africanus* (Lam.), and Sexual stimulation (aphrodisiacs) ⇒ *Ferula communis* L. show high confidence values, implying these medicinal materials are frequently used as aphrodisiacs. Specifically, *T. pungens* (Forssk.) Muell. Arg. and *Asparagus africanus* Lam. have high confidence and lift values, indicating their prominent role as aphrodisiacs. Conversely, Sexual stimulation (aphrodisiacs) ⇒ *Habenaria sp.* has a high lift value of 28.06 and a lower confidence value of 11.11, suggesting that *Habenaria sp.* is more specifically used for aphrodisiac purposes.

Regarding rabies infection, the rule Rabies ⇒ *Cucumis ficifolius* A. Rich. shows high confidence (43.75) but relatively low lift values (4.80). This indicates that *Cucumis ficifolius* A. Rich. is commonly used for treating rabies and several other conditions such as frequent miscarriage and sexual dysfunction. In contrast, Rabies ⇒ *Sida cuneifolia* Roxb. or *Sida ovata* Forssk. exhibits a high lift value of 10.52 but lower confidence (12.50), suggesting that these medicinal materials are more specifically used for treating rabies infection.

For conditions like frequent miscarriage and menorrhagia, the rules Frequent miscarriage ⇒ *Periploca linearifolia* A. Rich. & Quart.-Dill. and Menorrhagia ⇒ *Protea gaguedi* Gmel. exhibit high lift values (10.52 and 36.07, respectively), indicating their specific therapeutic roles in preventing miscarriage and treating menorrhagia. Further research into these medicinal materials could provide valuable insights into their efficacy.

Patterns observed for leprosy reveal that rules such as Leprosy ⇒ *Plumbago zeylanica* L., Leprosy ⇒ *Withania somnifera* (L.) Dunal, Leprosy ⇒ *Euclea schimperi* (DC.) Dandy, and Leprosy ⇒ *Capparis tomentosa* Lam. have high confidence and low lift values, suggesting these materials are commonly used to treat leprosy and other conditions. Conversely, Leprosy ⇒ *Sylvicapra grimmia*, Leprosy ⇒ *Withania somnifera* (L.) Dunal, and Leprosy ⇒ *Ranunculus multifidus* Forssk. have higher lift values and relatively lower confidence, indicating these medicinal materials are more specifically used to treat leprosy.

Similarly, other significant associations between diseases and medicinal materials can be discerned from Table 1. To substantiate these findings, additional in vitro and in vivo studies are needed to assess the effects of the medicinal materials and their extracts on the associated pathogens and diseases.

Network Visualization of Associations between Traditional Medicine and Diseases

Figure 5 presents a network diagram that visualizes the associations between 20 different diseases and their corresponding medicinal materials within the dataset used in this study. *Cucumis ficifolius* A. Rich. is shown as a large green circle, indicating its extensive use for treating various diseases. The large light blue square represents aphrodisiacs, highlighting the range of materials used for this purpose. Additionally, the diagram illustrates that leprosy and mental illness are linked to a significant number of medicinal materials, reflecting their diverse treatment approaches.

Figure 6 shows radar charts to effectively illustrate associations between medicinal materials and associated diseases. Leprosy was selected due to its extensive list of associated medicinal materials, making it a representative example for this visualization method. While these charts focus on leprosy, the same approach can be applied to other diseases. The radar charts show confidence values, which indicate the strength of the associations between specific medicinal materials and leprosy; lift values, which represent the specificity of these associations; and standardized values that facilitate comparative analysis. The charts show that *Sylvicapra grimmia*, *Maesa lanceolata* Forssk., and *Ranunculus multifidus* Forssk. have higher lift values relative to their confidence values, making them particularly specific to leprosy treatment. In contrast, *Plumbago zeylanica* L., *Withania somnifera* (L.) Dunal, *Euclea schimperi* (DC.) Dandy, and *Capparis tomentosa* Lam. display higher confidence values compared to their lift values, indicating these materials are more frequently used to treat leprosy but are also used to treat other conditions.

Exploring the Pharmacological Activity of *R. abyssinicus* Jacq. Phytochemicals via Target Identification, KEGG Pathways, GO Terms, and Network Analysis

In this study, we manually curated the phytochemicals in *R. abyssinicus* Jacq. From this curated list, we identified ten phytochemicals—emodin, chrysophanol, oleanolic acid, physcion, helminthosporin, lupeol, citreorosein, chrysophanein, and stigmastane-3,6-dione—that are present in the
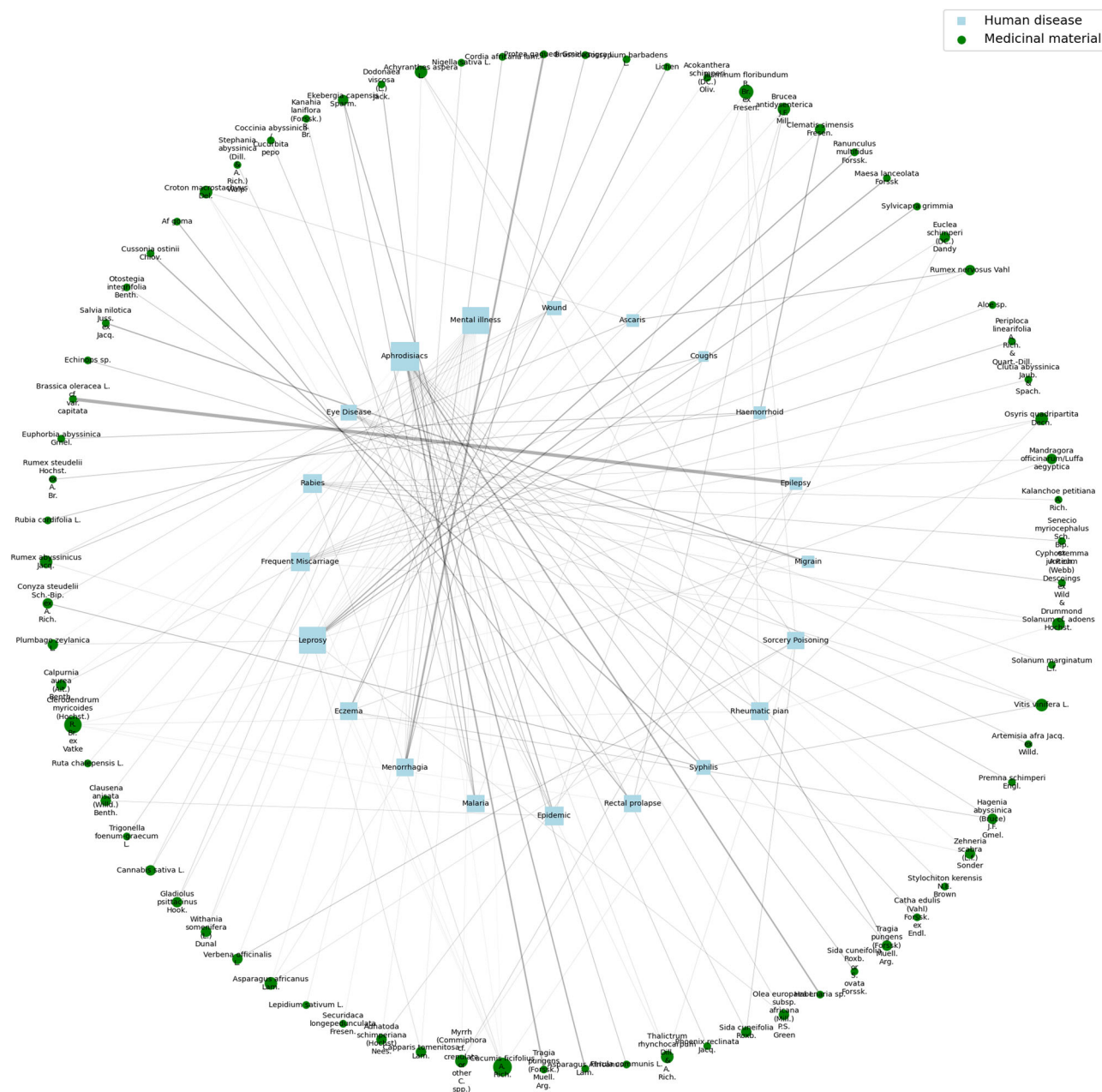
Fig. 5 Network diagram illustrating associations between diseases and medicinal materials. The diagram shows 20 diseases (light blue squares) and their associated medicinal materials (green circles). The size of the nodes reflects the degree of each node, and edge width indicates the the specificity of the association (measured by lift)

COCONUT database, which provides comprehensive data on compounds and their related human target genes/proteins. Utilizing this extensive compound-target data, we identified 756 human target genes/proteins associated with these phytochemicals.

KEGG pathway enrichment analysis of these targets revealed that they are significantly enriched in 196 KEGG pathways (adjusted P-value ≤ 0.05) (Supplementary Table S2 online). Figure 7A highlights the top 20 enriched KEGG pathways, involving 208 target genes/proteins. To visualize

these relationships, we constructed a network of targets and pathways using the Python NetworkX package version 2.5, as depicted in Fig. 7B. Key pathways identified include lipid metabolism, atherosclerosis, chemical carcinogenesis, cancer pathways, Kaposi's sarcoma-associated herpesvirus infection, AGE-RAGE signaling in diabetic complications, MAPK signaling, human cytomegalovirus infection, and C-type lectin receptor signaling. This KEGG enrichment analysis provides valuable insights into the potential therapeutic benefits of *R. abyssinicus* Jacq. phytochemicals.

A

Confidence (%)

B

Lift

C

Standardized confidence and lift
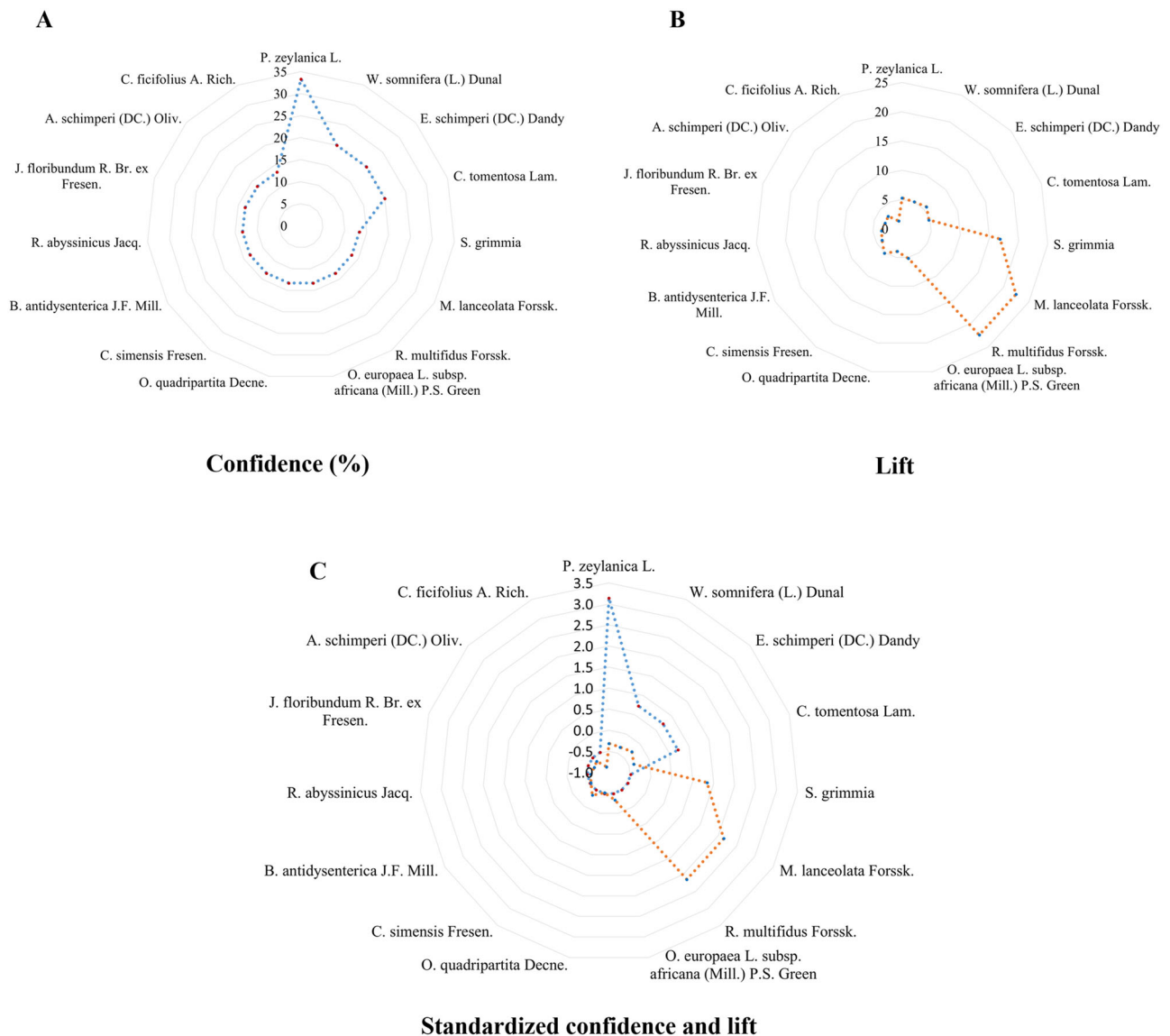
Fig. 6 Radar charts illustrating associations between medicinal materials and leprosy. **A** Radar chart of confidence values, indicating the reliability of associations between specific medicinal materials and leprosy. **B** Radar chart of lift values, showing the specificity of these associations, with higher values reflecting materials more specifically used for leprosy treatment. **C** Radar chart of standardized values for both confidence and lift, enabling comparative analysis

However, further research is needed to elucidate the specific mechanisms through which these phytochemicals exert their effects on the identified molecular targets.

GO analysis were performed to identify the biological processes associated with the 756 human target genes/proteins related to the phytochemicals from *R. abyssinicus* Jacq. These targets were significantly enriched in 918 biological processes (P-values ≤ 0.05) (Supplementary File S2 online). As depicted in Fig. 8A, the top 20 biological processes primarily involved proteolysis, cellular protein modification, dephosphorylation, estrogen metabolism, cortical cytoskeleton organization, and ras protein signal transduction. Additionally, a phytochemical-target-biological process network was constructed using Python's NetworkX package (version 2.5). This network, shown in Fig. 8B, highlights that 361 genes are predominantly associated with the top 20 biological processes.

Additionally, a network analysis was performed to identify diseases related to the target genes using the CODA network database employing RWR algorithm (see materials and methods). This analysis linked phytochemicals from *R. abyssinicus* Jacq. to a variety of diseases, including different types of cancers, metabolic and endocrine disorders (such as diabetes mellitus and hypertension), inflammatory conditions, immune system diseases, congenital malformations, respiratory disorders,
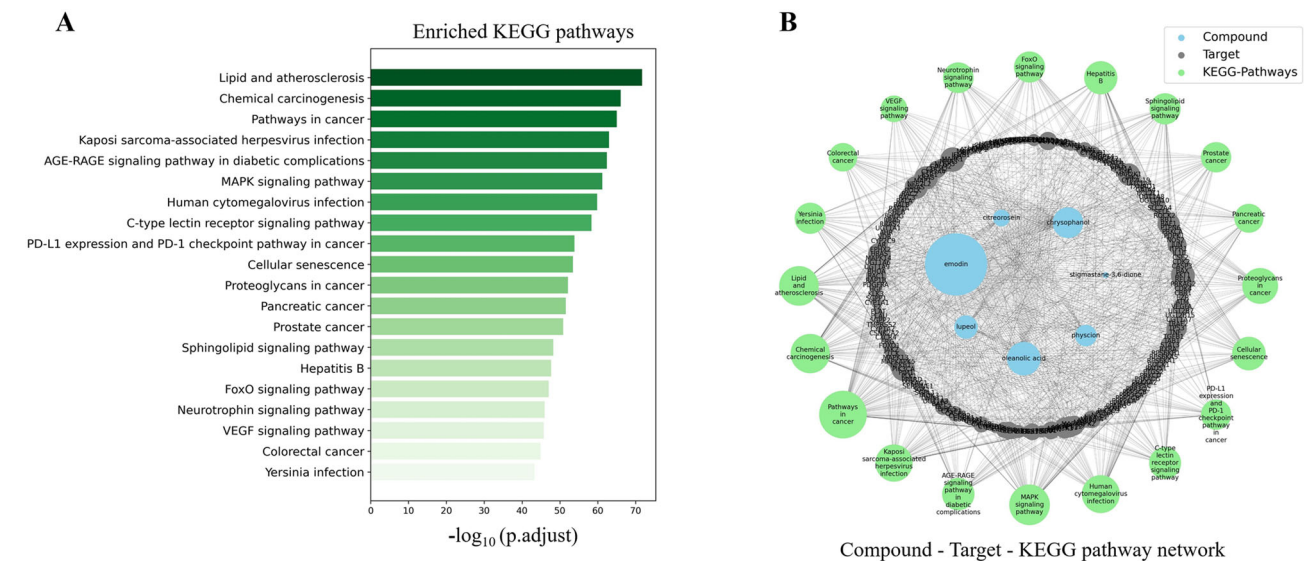
Fig. 7 KEGG Pathway Enrichment Analysis. **A** Bar graph showing the top 20 enriched pathways identified through KEGG analysis. **B** Phytochemical-target-pathway network created with Python NetworkX, depicting enriched pathways and their associated genes (Adjusted P ≤ 0.05)
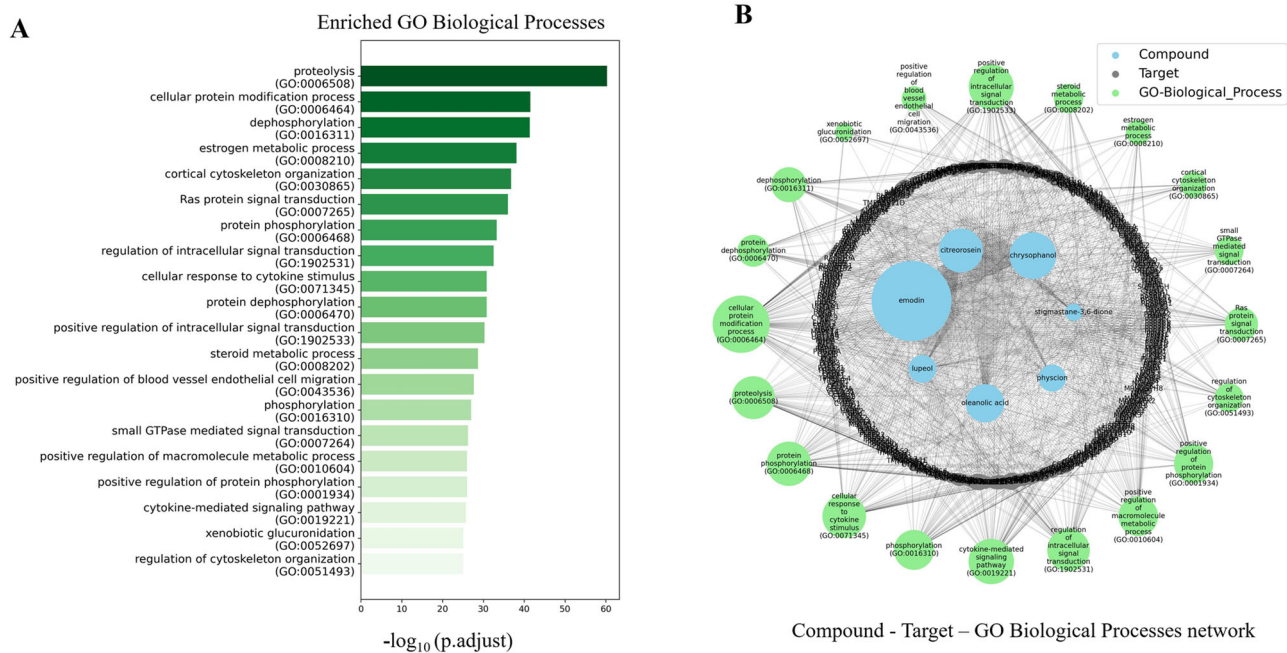

Fig. 8 Gene Ontology Enrichment Analysis. **A** Bar graph displaying the top 20 enriched biological processes identified through GO analysis. **B** Phytochemical-target-biological process network generated with Python NetworkX, illustrating enriched biological processes and the genes associated with the phytochemicals (Adjusted P ≤ 0.05)

and nervous system diseases. A comprehensive list of the related diseases is provided in Supplementary Table S3 online.

Many of the diseases identified through the network analysis correspond with the traditional therapeutic uses of *R. abyssinicus* Jacq. For instance, the anti-Alzheimer's effect of *R. abyssinicus* Jacq. is attributed to its isolated secondary metabolite, helmintosporin, which acts as a dual inhibitor of the enzymes AChE and BChE [55]. Additionally, crude extracts of *R. abyssinicus* demonstrate a broad spectrum of activities, including antibacterial antibacterial [56, 57], anticancer [57], antiviral [56], anti-inflammatory [54, 56], antioxidant [58], wound healing [54], antimalarial [59], diuretic, and analgesic [60] effects.

A

PPI network in CODA database

B

Hub targets of *R. abyssinicus* Jacq. Phytochemicals
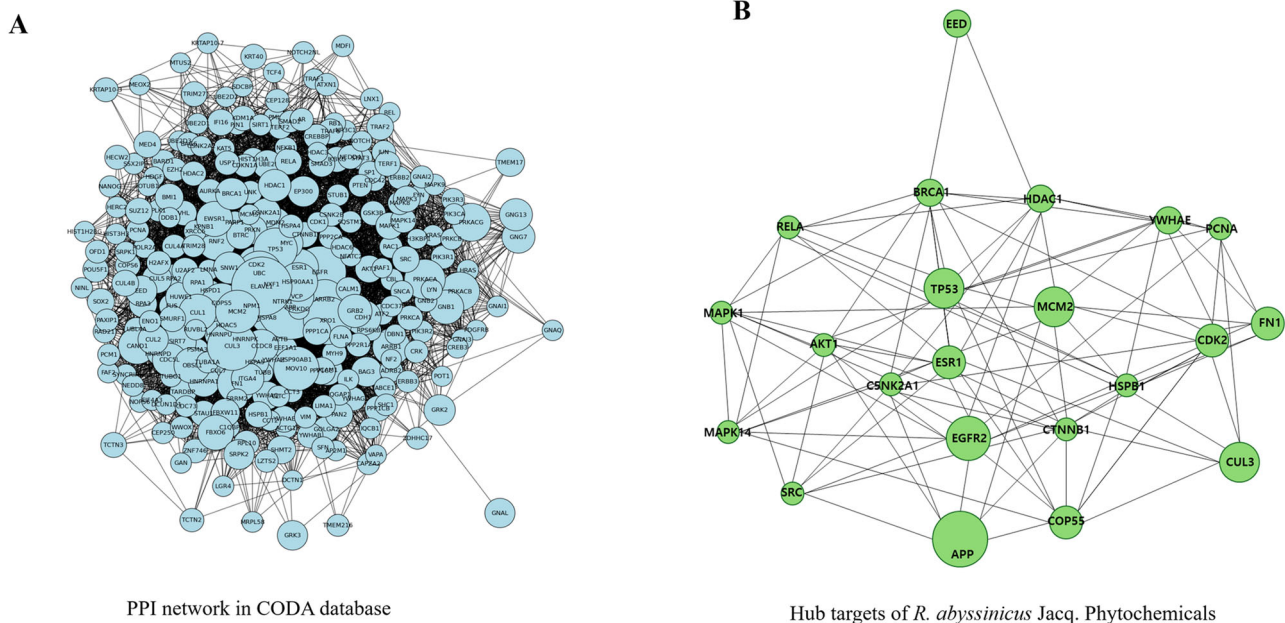
Fig. 9 PPI network and hub genes/proteins associated with *R. abyssinicus* Jacq. **A** PPI network constructed using the CODA platform, representing the overall network of protein-protein interactions.

B Network diagram of the 22 hub genes identified in the top 1% of centrality values from the CODA network, specifically related to the phytochemicals of *R. abyssinicus* Jacq.

One objective of this study was to validate the association rule mining results, specifically focusing on the association between wound and *R. abyssinicus* Jacq. To further investigate this association, we conducted in silico and network analysis to explore the molecular-level associations between the phytochemicals in *R. abyssinicus* Jacq. and wound-related conditions. Our analysis indicates that many phytochemicals in *R. abyssinicus* Jacq. are associated with disease categories related to wound, including inflammatory diseases, immune system disorders, and infectious diseases. Inflammation, marked by signs such as heat, redness, pain, swelling, increased body temperature, and fever, constitutes the initial stage of the wound healing process [61]. Infection is also a significant factor that can adversely affect wound healing [62]. These findings provide further support for the traditional use of *R. abyssinicus* Jacq. in treating wounds, aligning with the results obtained from the association rule mining.

PPI Network, Molecular Docking and Molecular Dynamics Simulations

From the CODA PPI network (Fig. 9A), we extracted hub targets associated with the phytochemicals in *R. abyssinicus* Jacq., as shown in Fig. 9B. These hub targets, identified through the PPI network, may hold therapeutic potential and offer insights into their clinical value [63]. The distribution of degree and eigenvector centralities for these hub targets was analyzed within the CODA PPI network, which includes 17,358 nodes. The top 1, 5, and 10% of nodes had

degree centrality values of 243, 101, and 67, respectively, and eigenvector centrality values of 0.0313, 0.0138, and 0.008, respectively. Notably, 22 targets associated with *R. abyssinicus* Jacq. were found in the top 1% for both degree and eigenvector centralities, as illustrated in Fig. 10A, B.These targets include APP, EGFR, CUL3, MCM2, TP53, COPS5, FN1, ESR1, CDK2, HDAC1, BRCA1, EED, CSNK2A1, AKT1, MAPK1, SRC, YWHAE, RELA, HSPB1, CTNNB1, MAPK14, and PCNA.

Several of these hub genes are linked to the wound healing process. For example, studies have shown that beta-amyloid precursor protein (APP) and its homolog, amyloid precursor-like protein 2 (APLP2), are expressed during skin wound repair in a mouse model of full-thickness skin excision [64]. The EGFR signaling pathway is known to play a crucial role in maintaining skin integrity and promoting wound healing [65]. Additionally, Estrogen Receptor 1 (ESR1) has been found to be enriched in patients with diabetic wounds (DWs) and regulates human skin fibroblasts [65]. The PPI network analysis supports our findings by identifying key hub targets linked to *R. abyssinicus* Jacq. phytochemicals, validating their potential therapeutic value, particularly in wound healing.

After identifying hub targets associated with phytochemicals from *R. abyssinicus* Jacq. using the CODA PPI network, we selected a subset of these targets and phytochemicals for further exploration. We performed structure-based molecular docking to investigate their interactions. The docking results indicated successful binding with low binding energies, suggesting interactions between the
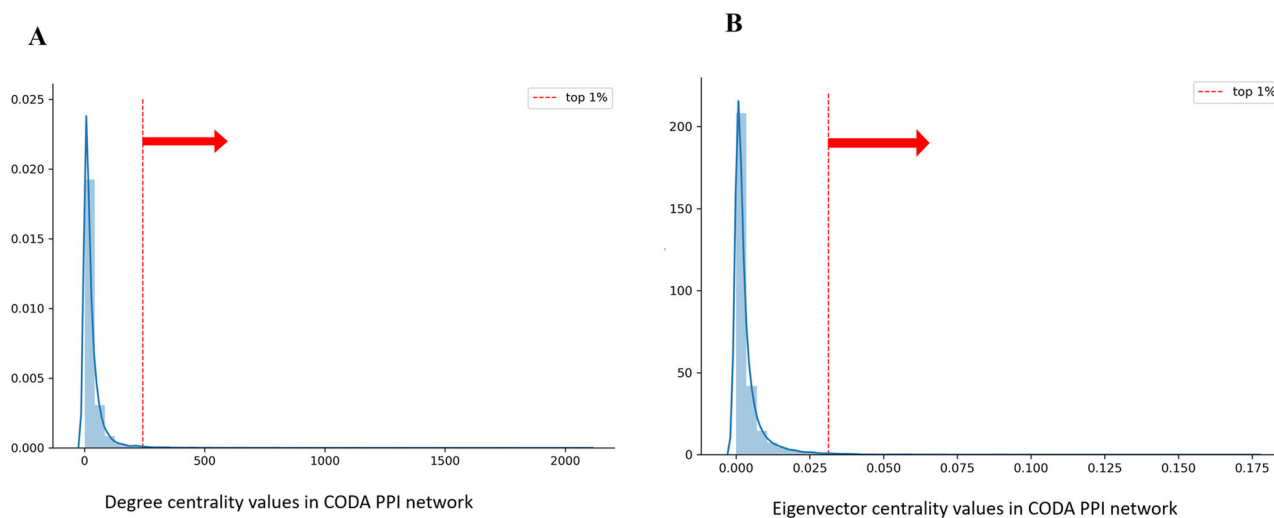
A

B

Fig. 10 Distribution of centrality values in the CODA network and targets associated with *R. abyssinicus* Jacq. **A** Distribution of degree centrality values across the CODA network, highlighting the top 1% of nodes. Among these, 22 targets associated with *R. abyssinicus* Jacq. were identified. **B** Distribution of eigenvector centrality values across the CODA network, focusing on the top 1% of nodes. The same 22 targets related to *R. abyssinicus* Jacq. were extracted from this subset

selected phytochemicals and the hub targets. Figure 11 shows 3D views of these interactions, and Table 2 provides details on binding affinities, interacting amino acid residues, docking centers, and docking sizes for the phytochemicals and their respective receptors.

The binding affinity energies and interactions between *R. abyssinicus* Jacq. phytochemicals and their respective receptors reveal crucial insights into the molecular mechanisms underlying their therapeutic potential. Generally, lower docking scores (more negative values) indicate stronger and more stable interactions. These interactions are primarily driven by hydrogen bonding, hydrophobic interactions, and electrostatic forces. Hydrogen bonds, particularly, enhance the stability and specificity of the ligand-receptor complex, while hydrophobic interactions contribute to the overall binding affinity by reducing the free energy of the ligand-receptor complex [66–68].

Emodin demonstrated the highest binding affinity with ESR1, followed by its interactions with EGFR. Physcione also showed a strong binding affinity with ESR1. These interactions typically involved key residues forming hydrogen bonds and hydrophobic interactions, which stabilized the ligand-receptor complexes and contributed to their high binding affinities. Oleanolic Acid exhibited significant binding affinities with CUL3 and APP. Similar to the other phytochemicals, the interactions were characterized by hydrogen bonds and hydrophobic interactions with key residues, enhancing the stability of the ligand-receptor complexes. Overall, the consistent presence of hydrogen bonds and hydrophobic interactions across these ligand-receptor complexes underlines their significance in determining binding affinity and stability, validating the potential therapeutic applications of these phytochemicals. The

docking output and MD simulation results confirmed stable interactions over time, supporting the robustness of these findings [66–68].

We conducted the MD simulation to evaluate the stable binding affinity of phytochemicals with their targets. Emodin, which demonstrated a favorable binding energy score (−8.9 kcal/mol) with the target ESR1 in docking studies, was chosen for the MD simulation. MD simulations provide a dynamic perspective on the interaction between ligands and their targets, complementing the static view offered by docking studies [69].

The RMSD parameter was utilized to examine the stability of the protein-ligand complex over 100 ns. RMSD is a measure of the average distance between atoms of superimposed proteins and is commonly used to assess the stability of protein structures and protein-ligand complexes in MD simulations [70]. The RMSD of the atoms in the ligand, ligand fit to protein backbone, and protein backbone exhibited similar patterns of fluctuation during most of the simulation period. The RMSD of ligand fit to protein backbone and protein backbone displayed an initial increase followed by stability throughout the simulation.

Notably, the RMSD of the ligand (Fig. 12, black) was slightly lower than that of the ligand fit to protein backbone (Fig. 12, green), indicating a conformational change of the target protein in the protein-ligand complex upon binding. This is a common observation in MD simulations, where ligands often induce conformational changes in the protein structure, enhancing the stability of the complex [71, 72]. The protein-ligand complex (Fig. 12, green) remained relatively stable throughout the simulation, indicating tight binding between the ligand and the receptor.
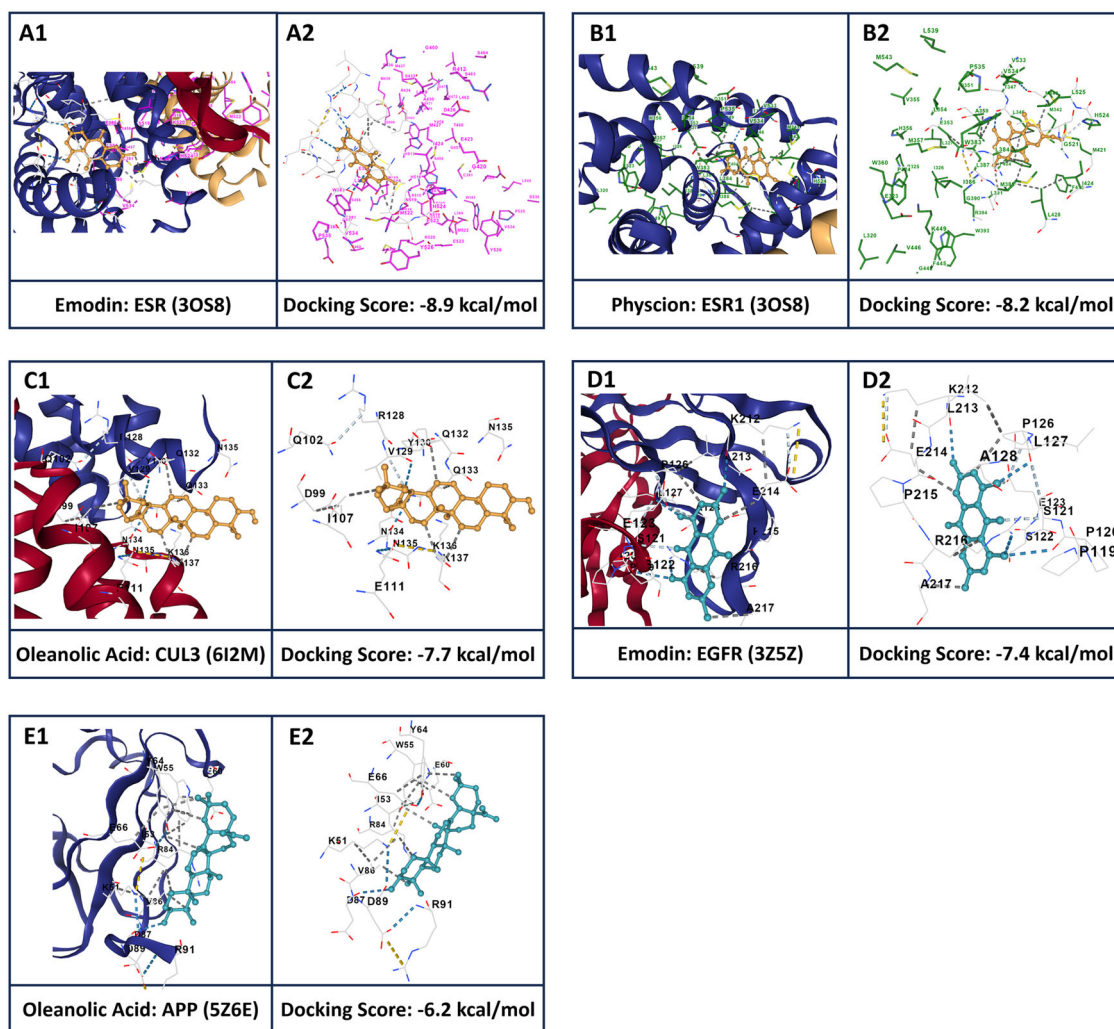
Fig. 11 Molecular docking analysis of select phytochemicals from *R. abyssinicus* Jacq. with their corresponding targets. (**A1**–**E1**) 3D visualization of interactions between selected phytochemicals and their corresponding targets. (**A2**–**E2**) 3D pose views of phytochemicals and their interacting residues, with targets removed to clearly show the interaction sites

Additionally, the Radius of gyration (Rg) analysis confirmed that the protein structures were largely unaffected by the binding region over the simulation period (Fig. 13). Rg measures the compactness of the protein structure and is another indicator of structural stability [71]. The consistent Rg values suggest that the protein maintained its structural integrity upon ligand binding, further supporting the stability of the protein-ligand complex.

Furthermore, the hydrogen bonds formed between the ligand and the protein play a crucial role in the stability of the complex. Hydrogen bonds contribute significantly to the binding energy and specificity of the interactions [73, 74]. The hydrophobic interactions, which reduce the free energy of the system, also play an essential role in maintaining the stability of the complex [75].

These findings suggest a stable interaction between the phytochemical and the target protein, supporting the potential therapeutic significance of the compound. The combined insights from docking studies and MD simulations provide a robust framework for understanding the molecular basis of the observed binding affinities, highlighting the importance of both hydrogen bonding and hydrophobic interactions in stabilizing the protein-ligand complexes [76, 77].

Overall, the integration of docking studies with MD simulations offers a comprehensive approach to validating the stability and potential efficacy of phytochemicals, such as Emodin, in targeting specific proteins. This approach underscores the therapeutic relevance of these compounds in traditional medicine and supports further experimental validation [78].

Conclusions

Our study aimed to identify and validate significant associations between human diseases and medicinal materials

Table 2 Binding affinity energies, interacting amino acid residues, docking center, and docking size for selected phytochemicals from *R. abyssinicus* Jacq. with their receptors

Phytochemical	Target (PDB ID)	Docking Score (Kcal/mol)	Interacting Amino Acid Residues	Docking Center (x, y, z)	Docking Size (x, y, z)
Emodin	ESR1 (3OS8)	−8.9	Chain B: TYR459, THR460, PHE461, LEU462, SER463, ARG515, SER518, ASN519, LYS520, MET522 Chain D: MET343, LEU345, LEU346, THR347, LEU349, ALA350, GLU353, TRP383, LEU384, LEU387, MET388, GLY390, LEU391, ARG394, PRO399, GLY400, LEU403, PHE404, ARG412, GLU423, ILE424, ASP426, MET427, LEU428, LEU429, ALA430, SER433, ARG436, HIS516, LYS520, GLY521, MET522, GLU523, HIS524, LEU525, VAL533	16, 17, −61	35, 32, 31
Physcion	ESR1 (3OS8)	−8.2	Chain D: MET343, LEU346, THR347, LEU349, ALA350, GLU353, TRP383, LEU384, LEU387, MET388, LEU391, ARG394, PHE404, MET421, ILE424, PHE425, LEU428, MET517, GLY521, MET522, HIS524, LEU525, VAL533, VAL534	27, 6, −62	28, 20, 20
Emodin	EGFR (3G5Z)	−7.4	Chain A: PRO119, PRO120, SER121, SER122, GLU123, LEU125, TYR186, PHE209, ARG211, ASN212, GLU213. Chain B: PRO126, LEU127, ALA128, PRO129, GLY130, CYS131, GLY132, ASP133, THR134, THR135, GLY136, VAL139, THR140, LEU141, PRO187, SER188, TRP191, PRO192, LYS212, LEU213, GLU214, PRO215, ARG216, ALA217	11, 39, 50	19, 25, 19
Oleanolic Acid	CUL3 (6I2M)	−7.7	Chain A: GLY41, ALA42, SER43, GLU44, ASP99, GLN102, ILE103, GLY104, SER105, ILE107, THR108, GLU111, ASN134, ASN135, LYS136, LYS137, SER140 Chain B: VAL117, ARG120, MET124, ASP127, ARG128, VAL129, TYR130, VAL131, GLN132, GLN133, ASN135, VAL136, ASN138, VAL139, TYR140	−29, −9, 47	23, 23, 23
Oleanolic Acid	APP (5Z6E)	−6.3	Chain A: VAL27, LYS51, ILE53, TRP55, GLU60, TYR64, GLU66, ARG84, VAL86, ASP87, ASP89, THR90, ARG91	6, 35, 2	23, 23, 23
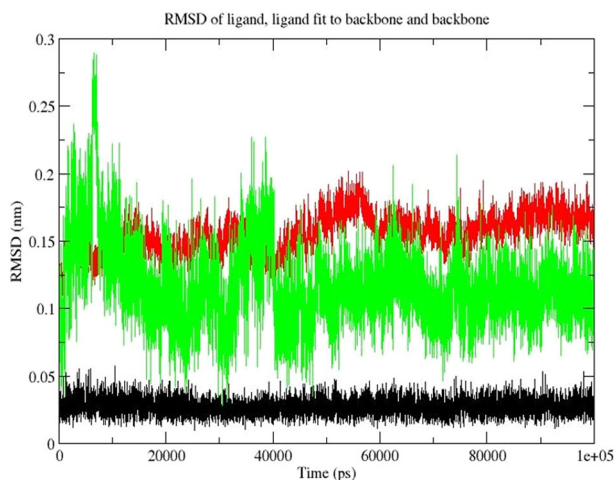
Fig. 12 Root Mean Square Deviation (RMSD) plots of ligand and target protein backbone. RMSD plots showing the deviation of the ligand (emodin) (black), the target protein backbone (ESR1) (red), and the ligand fit to the backbone (green) over 100 ns of molecular dynamics simulation
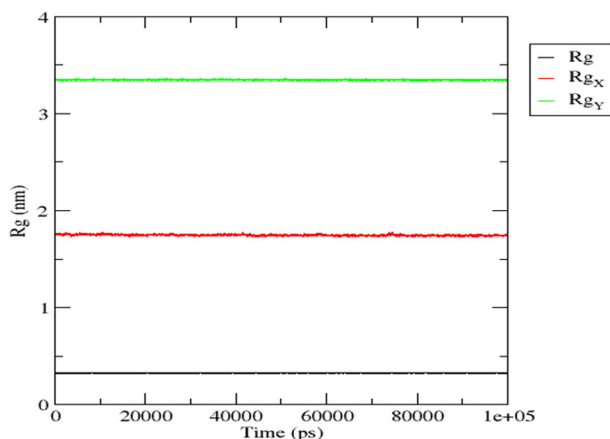

Fig. 13 Radius of gyration (Rg) plots. Plots of the radius of gyration (Rg, in nm) for the ligand (emodin) (Rg), the target protein backbone (ESR1) (RgX), and the entire system (RgY) over 100 ns of simulation

used in Ethiopian traditional medicine prescriptions, ultimately aiming to identify reliable therapeutic medicines for common human diseases. Through association rule mining, we successfully identified notable associations, including a significant association between *R. abyssinicus* Jacq. and wound healing.

To further support these findings, we conducted in silico analysis to explore the molecular-level associations between the phytochemicals in *R. abyssinicus* Jacq. and various therapeutic targets, pathways, and biological processes. This analysis revealed 756 associated targets enriched across diverse KEGG pathways and GO terms, indicating potential therapeutic effects against a broad spectrum of

diseases, including cancer, metabolic disorders, endocrine diseases, inflammation, immune system diseases, congenital malformations, respiratory issues, and neurological conditions. Network analysis using the CODA network highlighted key hub target genes linked with *R. abyssinicus* Jacq.'s phytochemicals, emphasizing their role in wound healing. Molecular docking and molecular dynamics simulations further supported these findings by confirming stable binding interactions between the phytochemicals and the identified hub targets.

In summary, our in silico and network analysis robustly validate the association rule mining results and the traditional therapeutic applications of *R. abyssinicus* Jacq. in wound treatment. However, to fully confirm these results, controlled experimental studies on the pharmacological effects of *R. abyssinicus* Jacq. phytochemicals are necessary [37].

Compliance with Ethical Standards

Conflict of Interest The authors declare no competing interests.

Publisher's note Springer Nature remains neutral with regard to jurisdictional claims in published maps and institutional affiliations.

Abbreviations

CODA	Context-Oriented Directed Associations

COCONUT	Compound Combination-Oriented Natural Product Database with Unified Terminology
ETM-DB	Integrated Ethiopian Traditional Herbal Medicine and Phytochemicals Database
GO	Gene Ontology
GROMACS	Groningen Machine for Chemical Simulations
KEGG	Kyoto Encyclopedia of Genes and Genomes
MD	Molecular Dynamics
ML/AI	Machine Learning/Artificial Intelligence
NPT	Constant Number of Particles, Pressure, and Temperature
NVT	Constant Number of Particles, Volume, and Temperature
PPI	Protein-Protein Interaction
QSAR	Quantitative Structure-Activity Relationship
RWR	Random-Walk with Restart
Rg	Radius of Gyration
RMSD	Root Mean Square Deviation
TCAM	Traditional, Complementary and Alternative Medicine
TM	Traditional Medicine
VS	Virtual Screening
LBDD	Ligand-Based Drug Design
GSEA	Gene Set Enrichment Analysis

References

1. Ekor, M. (2014). The growing use of herbal medicines: Issues relating to adverse reactions and challenges in monitoring safety. *Frontiers in Pharmacology*, 4, 177. https://doi.org/10.3389/fphar.2013.00177.

2. Che, C. T., George, V., Ijinu, T. P., Pushpangadan, P., & Andrae-Marobela, K. (2017). Traditional Medicine. In *Pharmacognosy: fundamentals, applications and strategy* (pp. 15–30). Elsevier Inc. https://doi.org/10.1016/B978-0-12-802104-0.00002-0.

3. Kayne, S. B. (2010). Introduction to traditional medicine. In *Traditional medicine: A global perspective* (pp. 25–39). Pharmaceutical Press

4. van den Bosch, Matilda, & William Bird (2018). *Oxford textbook of nature and public health: The role of nature in improving the health of a population*. Oxford University Press. https://doi.org/10.1093/med/9780198725916.001.0001.

5. Yoo, S., Ha, S., Shin, M., Noh, K., Nam, H., & Lee, D. (2018). A data-driven approach for identifying medicinal combinations of natural products. *IEEE Access*, 6, 58106–58118. https://doi.org/10.1109/ACCESS.2018.2874089.

6. Bultum, L. E., Woyessa, A. M., & Lee, D. (2019). ETM-DB: Integrated Ethiopian traditional herbal medicine and phytochemicals database. *BMC Complementary and Alternative Medicine*, 19(1), 1–11. https://doi.org/10.1186/s12906-019-2634-1.

7. Sadybekov, A. V., & Katritch, V. (2023). Computational approaches streamlining drug discovery. *Nature*, 616, 673–685. https://doi.org/10.1038/s41586-023-05905-z.

8. Kitchen, D. B., Decornez, H., Furr, J. R., & Bajorath, J. (2004). Docking and scoring in virtual screening for drug discovery: Methods and applications. *Nature Reviews Drug Discovery*, 3(11), 935–949.

9. Lu, W., Zhang, R., Jiang, H., Zhang, H., & Luo, C. (2018). Computer-aided drug design in epigenetics. *Frontier in Chemistry*, 6, 57. https://doi.org/10.3389/fchem.2018.00057.

10. Niazi, S. K., & Mariam, Z. (2023). Computer-aided drug design and drug discovery: A prospective analysis. *Pharmaceuticals*, 17(1). https://doi.org/10.3390/ph17010022.

11. Hughes, J. P., Rees, S. S., Kalindjian, S. B., & Philpott, K. L. (2011). Principles of early drug discovery. *British Journal of Pharmacology*, 162(6), 1239–1249. https://doi.org/10.1111/j.1476-5381.2010.01127.x.

12. Cherkasov, A., Muratov, E. N., Fourches, D., Varnek, A., Baskin, I. I., Cronin, M., Dearden, J., Gramatica, P., Martin, Y. C., Todeschini, R., Consonni, V., Kuz'Min, V. E., Cramer, R., Benigni, R., Yang, C., Rathman, J., Terfloth, L., Gasteiger, J., Richard, A., & Tropsha, A. (2014). QSAR modeling: Where have you been? Where are you going to? *Journal of Medicinal Chemistry*, 57(12), 4977–5010. https://doi.org/10.1021/jm4004285.

13. Sanchez-Lengeling, B., & Aspuru-Guzik, A. (2018). Inverse molecular design using machine learning: Generative models for matter engineering. *Science*, 361(6400), 360–365. https://doi.org/10.1126/science.aap7885.

14. Walters, W. P., & Barzilay, R. (2021). Critical assessment of AI in drug discovery. *Expert Opinion Drug Discovery*, 16(9), 937–947.

15. Witten, I. H., Frank, E., Hall, M. A., & Pal, C. J. (2016). *Data mining: Practical machine learning tools and techniques* (4th ed.). Morgan Kaufmann

16. Yang, Y., Adelstein, S. J., & Kassis, A. I. (2009). Target discovery from data mining approaches. *Drug Discovery Today*, 14(3), 147–154. https://doi.org/10.1016/j.drudis.2008.12.005.

17. Kantardzic, M. (2011). Data mining: Concepts, models, methods, and algorithms. Wiley.

18. Agrawal, R., Imieliński, T., & Swami, A. (1993). Mining association rules between sets of items in large databases. *ACM SIGMOD Record*, 22(2), 207–216. https://doi.org/10.1145/170036.170072.

19. Valdeolivas, A., Tichit, L., Navarro, C., Perrin, S., Odelin, G., Levy, N., Cau, P., Remy, E., & Baudot, A. (2019). Random walk with restart on multiplex and heterogeneous biological networks. *Bioinformatics*, 35(3), 497–505. https://doi.org/10.1093/bioinformatics/bty637.

20. Kassaye, K., Amberbir, A., Getachew, B., & Mussema, Y. (2007). A historical overview of traditional medicine practices and policy in Ethiopia. *The Ethiopian Journal of Health Development*, 20(2). https://doi.org/10.4314/ejhd.v20i2.10023.

21. WHO. (2019). *WHO global report on traditional and complementary medicine*. World Health Organization

22. Hailu, F., Cherie, A., Gebreyohannis, T., & Hailu, R. (2020). Determinants of traditional medicine utilization for children: A parental level study in Tole District, Oromia, Ethiopia. *BMC Complementary Medicine Therapies*, 20(1), 125. https://doi.org/10.1186/s12906-020-02928-1.

23. Negasu, G., Banchiamlak, N., & Mihirat, M. (2016). Composition, distribution, and economic importance of insect pests of prioritized aromatic plants in some growing areas of Ethiopia. *International Journal Advanced Biological and Biomedical Research*, 4(1), 1–9. https://doi.org/10.18869/IJABBR.2016.1.

24. Bekele, E. (2007). Study on actual situation of medicinal plants in Ethiopia. *Japan Association for International Collaboration of Agriculture and Forestry*, 4(3), 1–5

25. Fullas, F. (2001). *Ethiopian traditional medicine: Common medicinal plants in perspective*. F. Fullas.

26. Abebe, D. S. (2001). The role of medicinal plants in health care coverage of Ethiopia: The possible benefits of integration. In Proceedings. Retrieved from https://api.semanticscholar.org/CorpusID:131234921.

27. Giday, M., Asfaw, Z., & Woldu, Z. (2009). Medicinal plants of the Meinit ethnic group of Ethiopia: An ethnobotanical study. *Journal of Ethnopharmacology*, *124*(3), 513–521.

28. Suleman, S., & Alemu, T. (2012). A survey on utilization of ethnomedicinal plants in Nekemte town, East Wellega (Oromia), Ethiopia. *Journal of Herbs, Spices & Medicinal Plants*, *18*(1), 34–57. https://doi.org/10.1080/10496475.2011.645188.

29. Mukherjee, P. K., Banerjee, S., Kar, A., & Chanda, J. (2020). Drugs from our ancestors: Tradition to innovation. In *Herbal medicine in India: Indigenous knowledge, practice, innovation and its value* (pp. 263–280). Springer Nature Singapore

30. Mukherjee, P. K., Banerjee, S., Gupta, B. D., & Kar, A. (2022). Evidence-based validation of herbal medicine: Translational approach. In *Evidence-based validation of herbal medicine* (pp. 1–41). Elsevier

31. Pankhurst, R. K. P. (1990). *An introduction to the medical history of Ethiopia*. Red Sea Press

32. Abebe, D., & Ayehu, A. (1993). *Medicinal plants and enigmatic health practices of northern ethiopia* (pp. 419–431). Addis Ababa: B.S.P.E.

33. Limenih, Y., Umer, S., & Wolde-Mariam, M. (2015). Ethnobotanical study on traditional medicinal plants in Dega Damot Woreda, Amhara Region, North Ethiopia. Retrieved from https://api.semanticscholar.org/CorpusID:44691639.

34. Teklehaymanot, T., & Giday, M. (2007). Ethnobotanical study of medicinal plants used by people in Zegie Peninsula, Northwestern Ethiopia. *Journal of Ethnobiology Ethnomedicine*, *3*(1), 12 https://doi.org/10.1186/1746-4269-3-12.

35. Geyid, A., Abebe, D., Debella, A., Makonnen, Z., Aberra, F., Teka, F., Kebede, T., Urga, K., Yersaw, K., Biza, T., Mariam, B. H., & Guta, M. (2005). Screening of some medicinal plants of Ethiopia for their anti-microbial properties and chemical profiles. *Journal of Ethnopharmacology*, *97*(3), 421–427. https://doi.org/10.1016/j.jep.2004.08.021.

36. Ogata, H., Goto, S., Sato, K., Fujibuchi, W., Bono, H., & Kanehisa, M. (1999). KEGG: Kyoto encyclopedia of genes and genomes. *Nucleic Acids Research*, *27*(1), 29–34. https://doi.org/10.1093/nar/27.1.29.

37. Gene Ontology Consortium, The Gene Ontology (GO) database and informatics resource. *Nucleic Acids Research*, *32*(suppl_1), D258–D261. https://doi.org/10.1093/nar/gkh036.

38. Larose, D. T., & Larose, C. D. (2014). *Discovering knowledge in data: An introduction to data mining*. Wiley

39. Garg, A. (2018). *Complete guide to Association Rules. Algorithms that help you shop faster and smarter*. Towards Data Science. Retrieved from https://towardsdatascience.com/association-rules-2-aa9a77241654

40. Hornik, K., Grün, B., & Hahsler, M. (2005). Arules—A computational environment for mining association rules and frequent item sets. *J. Stat. Softw*, *14*(15), 1–25.

41. Agrawal, R., & Srikant, R. (1994). Fast algorithms for mining association rules. In *Proceedings of the 20th International Conference on Very Large Data Bases (VLDB)* (pp. 487–499). Santiago de Chile: Morgan Kaufmann

42. Stephen, F. (2004). *Show me the numbers: Designing tables and graphs to enlighten*. Analytics Press.

43. Mukherjee, P. K., Banerjee, S., & Kar, A. (2021). Molecular combination networks in medicinal plants: Understanding synergy by network pharmacology in Indian traditional medicine.

Phytochemistry Reviews, *20*(4), 693–703. https://doi.org/10.1007/s11101-020-09730-4.

44. Yu, H., Jung, J., Yoon, S., Kwon, M., Bae, S., Yim, S., Lee, J., Kim, S., Kang, Y., & Lee, D. (2017). CODA: Integrating multi-level context-oriented directed associations for analysis of drug effects. *Scientific Reports*, *7*(1), 7519 https://doi.org/10.1038/s41598-017-07448-6.

45. Fang, Z., Liu, X., & Peltz, G. (2023). GSEApy: A comprehensive package for performing gene set enrichment analysis in Python. *Bioinformatics*, *39*(1), btac757. https://doi.org/10.1093/bioinformatics/btac757.

46. Kim, S., Chen, J., Cheng, T., Gindulyte, A., He, J., He, S., Li, Q., Shoemaker, B. A., Thiessen, P. A., Yu, B., Zaslavsky, L., Zhang, J. & Bolton, E. E. (2023). PubChem 2023 update. *Nucleic Acids Research*, *51*(D1), D1373–D1380. https://doi.org/10.1093/nar/gkac956.

47. Liu, Y., Grimm, M., Dai, W.-T., Hou, M.-C., Xiao, Z.-X., & Cao, Y. (2020). CB-Dock: A web server for cavity detection-guided protein-ligand blind docking. *Acta Pharmacologica Sinica*, *41*(1), 138–144. https://doi.org/10.1038/s41401-019-0228-6.

48. Abraham, M. J., Murtola, T., Schulz, R., Páll, S., Smith, J. C., Hess, B., & Lindahl, E. (2015). GROMACS: High performance molecular simulations through multi-level parallelism from laptops to supercomputers. *SoftwareX*, *1–2*, 19–25. https://doi.org/10.1016/j.softx.2015.06.001.

49. Zoete, V., Cuendet, M. A., Grosdidier, A., & Michielin, O. (2011). SwissParam: A fast force field generation tool for small organic molecules. *Journal of Computational Chemistry*, *32*(11), 2359–2368. https://doi.org/10.1002/jcc.21816.

50. Bjelkmar, P., Larsson, P., Cuendet, M. A., Hess, B., & Lindahl, E. (2010). Implementation of the CHARMM force field in GROMACS: analysis of protein stability effects from correction maps, virtual interaction sites, and water models. *Journal of Chemical Theory Computation*, *6*(2), 459–466. https://doi.org/10.1021/ct900549r.

51. Golo, V. L., & Shaǐtan, K. V. (2002). Dynamic attractor for the Berendsen thermostat and the slow dynamics of biomacromolecules. *Biofizika*, *47*(4), 611–617.

52. Tuble, S. C., Anwar, J., & Gale, J. D. (2004). An approach to developing a force field for molecular simulation of martensitic phase transitions between phases with subtle differences in energy and structure. *Journal of the American Chemical Society*, *126*(1), 396–405. https://doi.org/10.1021/ja0356131.

53. Grace Development Team. (1991-2008). Grace: GRaphing, advanced computation and exploration of data (Version 5.1.22). Retrieved from http://plasma-gate.weizmann.ac.il/Grace/.

54. Mulisa, E., Asres, K., & Engidawork, E. (2015). Evaluation of wound healing and anti-inflammatory activity of the rhizomes of *Rumex abyssinicus* J. (Polygonaceae) in mice. *BMC Complementary and Alternative Medicine*, *15*(1), 1–10. https://doi.org/10.1186/s12906-015-0878-y.

55. Augustin, N., Nuthakki, V. K., Abdullaha, M., Hassan, Q. P., Gandhi, S. G., & Bharate, S. B. (2020). Discovery of Helminthosporin, an Anthraquinone Isolated from Rumex abyssinicus Jacq as a Dual Cholinesterase Inhibitor. *ACS Omega*, *5*(3), 1616–1624. https://doi.org/10.1021/acsomega.9b03693.

56. Getie, M., Gebre-Mariam, T., Rietz, R., Höhne, C., Huschka, C., Schmidtke, M., Abate, A., & Neubert, R. H. H. (2003). Evaluation of the anti-microbial and anti-inflammatory activities of the medicinal plants Dodonaea viscosa, Rumex nervosus, and Rumex abyssinicus. *Fitoterapia*, *74*(1), 139–143. https://doi.org/10.1016/S0367-326X(02)00315-5.

57. Tamokou, J., de, D., Chouna, J. R., Fischer-Fodor, E., Chereches, G., Barbos, O., Damian, G., Benedec, D., Duma, M., Efouet, A. P. N., Wabo, H. K., Kuiate, J. R., Mot, A., & Silaghi-Dumitrescu, R. (2013). Anticancer and antimicrobial activities of some

antioxidant-rich Cameroonian medicinal plants. *PLoS ONE*, *8*(2), e55880.

58. Mohammed, S. A., Panda, R. C., Madhan, B., & Demessie, B. A. (2017). Extraction of bio-active compounds from Ethiopian plant material *Rumex abyssinicus* (mekmeko) root—A study on kinetics, optimization, antioxidant, and antibacterial activity. *Journal of the Taiwan Institute Chemical Engineers*, *75*, 228–239. https://doi.org/10.1016/j.jtice.2017.03.004.

59. Muganga, R., Angenot, L., Tits, M., & Frédérich, M. (2010). Antiplasmodial and cytotoxic activities of Rwandan medicinal plants used in the treatment of malaria. *J. Ethnopharmacol.*, *128*(1), 52–57. https://doi.org/10.1016/j.jep.2009.12.023.

60. Mekonnen, T., Urga, K., & Engidawork, E. (2010). Evaluation of the diuretic and analgesic activities of the rhizomes of *Rumex abyssinicus* Jacq in mice. *Journal of Ethnopharmacology*, *127*(2), 433–439. https://doi.org/10.1016/j.jep.2009.10.020.

61. Collier, M. (2003). Understanding wound inflammation. *Nursing Times*, *99*(25), 63–64.

62. Guo, S., & Dipietro, L. A. (2010). Factors affecting wound healing. *Journal of Dental Research*, *89*(3), 219–229. https://doi.org/10.1177/0022034509359125.

63. Xiong, Y., You, W., Wang, R., Peng, L., & Fu, Z. (2017). Prediction and validation of hub genes associated with colorectal cancer by integrating PPI network and gene expression data. *BioMed Research International*, *2017*, 2421459 https://doi.org/10.1155/2017/2421459.

64. Kummer, C., Wehner, S., Quast, T., Werner, S., & Herzog, V. (2002). Expression and potential function of beta-amyloid precursor proteins during cutaneous wound repair. *Experimental Cell Research*, *280*(2), 222–232. https://doi.org/10.1006/excr.2002.5631.

65. Bodnar, R. J. (2013). Epidermal growth factor and epidermal growth factor receptor: The Yin and Yang in the treatment of cutaneous wounds and cancer. *Advances in Wound Care*, *2*(1), 24–29. https://doi.org/10.1089/wound.2011.0326.

66. Davis, I. W., Leaver-Fay, A., Chen, V. B., Block, J. N., Kapral, G. J., Wang, X., Murray, L. W., Arendall, III, W. B., Snoeyink, J., Richardson, J. S., & Richardson, D. C. (2007). MolProbity: All-atom contacts and structure validation for proteins and nucleic acids. *Nucleic Acids Research*, *35*(suppl_2), W375–W383. https://doi.org/10.1093/nar/gkm216.

67. Forli, S., Huey, R., Pique, M. E., Sanner, M. F., Goodsell, D. S., & Olson, A. J. (2016). Computational protein–ligand docking and virtual drug screening with the AutoDock suite. *Nature Protocols*, *11*(5), 905–919. https://doi.org/10.1038/nprot.2016.051.

68. Trott, O., & Olson, A. J. (2010). AutoDock Vina: Improving the speed and accuracy of docking with a new scoring function, efficient optimization, and multithreading. *Journal of Computational Chemistry*, *31*(2), 455–461. https://doi.org/10.1002/jcc.21334.

69. Hollingsworth, S. A., & Dror, R. O. (2018). Molecular dynamics simulation for all. *Neuron*, *99*(6), 1129–1143. https://doi.org/10.1016/j.neuron.2018.08.011.

70. Wu, N., Zhang, R., Peng, X., Fang, L., Chen, K., & Jestilä, J. S. (2024). Elucidation of protein–ligand interactions by multiple trajectory analysis methods. *Physical Chemistry Chemical Physics*, *26*(8), 6903–6915.

71. Borjian Boroujeni, M., Shahbazi Dastjerdeh, M., Shokrgozar, M., Rahimi, H., & Omidinia, E. (2021). Computational driven molecular dynamics simulation of keratinocyte growth factor behavior at different pH conditions. *Informatics Medicine Unlocked*, *23*, 100514 https://doi.org/10.1016/j.imu.2021.100514.

72. Lindorff-Larsen, K., Piana, S., Palmo, K., Maragakis, P., Klepeis, J. L., Dror, R. O., & Shaw, D. E. (2010). Improved side-chain torsion potentials for the Amber ff99SB protein force field. *Proteins*, *78*(8), 1950–1958. https://doi.org/10.1002/prot.22711.

73. Malik, F. K., & Guo, J.-T. (2022). Insights into protein-DNA interactions from hydrogen bond energy-based comparative protein-ligand analyses. *Proteins*, *90*(6), 1303–1314. https://doi.org/10.1002/prot.26313.

74. Chen, D., Oezguen, N., Urvil, P., Ferguson, C., Dann, S. M., & Savidge, T. C. (2016). Regulation of protein-ligand binding affinity by hydrogen bond pairing. *Science Advances*, *2*(3), e1501240 https://doi.org/10.1126/sciadv.1501240.

75. Laskowski, R. A., Luscombe, N. M., Swindells, M. B., & Thornton, J. M. (1996). Protein clefts in molecular recognition and function. *Protein Science*, *5*(12), 2438–2452. https://doi.org/10.1002/pro.5560051206.

76. Jorgensen, W. L. (2009). Efficient drug lead discovery and optimization. *Accounts of Chemical Research*, *42*(6), 724–733. https://doi.org/10.1021/ar800236t.

77. Karplus, M., & Kuriyan, J. (2005). Molecular dynamics and protein function. *Proceedings of the National Academy of Science of the United States of America*, *102*(19), 6679–6685. https://doi.org/10.1073/pnas.0408930102.

78. Shoichet, B. K. (2004). Virtual screening of chemical libraries. *Nature*, *432*(7019), 862–865. https://doi.org/10.1038/nature03197.